Plant Molecular Biology (2018) 96:509–529
https://doi.org/10.1007/s11103-018-0714-0

# Comprehensive transcriptome analyses correlated with untargeted metabolome reveal differentially expressed pathways in response to cell wall alterations

**Nathan T. Reem[1] · Han-Yi Chen[5,6] · Manhoi Hur[2] · Xuefeng Zhao[3,4] · Eve Syrkin Wurtele[2] · Xu Li[5,6] · Ling Li[2,7] · Olga Zabotina[1]**

Received: 12 October 2017 / Accepted: 25 February 2018 / Published online: 3 March 2018
© Springer Science+Business Media B.V., part of Springer Nature 2018

## Abstract

***Key message*** **This research provides new insights into plant response to cell wall perturbations through correlation of transcriptome and metabolome datasets obtained from transgenic plants expressing cell wall-modifying enzymes.**

**Abstract** Plants respond to changes in their cell walls in order to protect themselves from pathogens and other stresses. Cell wall modifications in *Arabidopsis thaliana* have profound effects on gene expression and defense response, but the cell signaling mechanisms underlying these responses are not well understood. Three transgenic Arabidopsis lines, two with reduced cell wall acetylation (AnAXE and AnRAE) and one with reduced feruloylation (AnFAE), were used in this study to investigate the plant responses to cell wall modifications. RNA-Seq in combination with untargeted metabolome was employed to assess differential gene expression and metabolite abundance. RNA-Seq results were correlated with metabolite abundances to determine the pathways involved in response to cell wall modifications introduced in each line. The resulting pathway enrichments revealed the deacetylation events in AnAXE and AnRAE plants induced similar responses, notably, upregulation of aromatic amino acid biosynthesis and changes in regulation of primary metabolic pathways that supply substrates to specialized metabolism, particularly those related to defense responses. In contrast, genes and metabolites of lipid biosynthetic pathways and peroxidases involved in lignin polymerization were downregulated in AnFAE plants. These results elucidate how primary metabolism responds to extracellular stimuli. Combining the transcriptomics and metabolomics datasets increased the power of pathway prediction, and demonstrated the complexity of pathways involved in cell wall-mediated signaling.

**Keywords** *Arabidopsis thaliana* · Cell wall signaling · Metabolomics · Systems biology · Transcriptomics

## Introduction

The plant cell wall is a dynamic structure that protects cells against environmental stresses and participates in signal transduction. Due to their sessile nature, plant survival depends on effective protection and constant surveillance

**Electronic supplementary material** The online version of this article (https://doi.org/10.1007/s11103-018-0714-0) contains supplementary material, which is available to authorized users.

✉ Olga Zabotina
zabotina@iastate.edu

[1] Department of Biochemistry, Biophysics and Molecular Biology, Iowa State University, Ames, USA

[2] Department of Genetics, Developmental and Cell Biology, Iowa State University, Ames, USA

[3] Laurence H. Baker Center for Bioinformatics and Biological Statistics, Iowa State University, Ames, USA

[4] Present Address: Information Technology, College of Liberal Arts and Sciences, Iowa State University, Ames, USA

[5] Plants for Human Health Institute, North Carolina State University, Kannapolis, USA

[6] Department of Plant and Microbial Biology, North Carolina State University, Raleigh, USA

[7] Department of Biological Sciences, Mississippi State University, Starkville, USA

for danger. Complex cell wall structures evolved as a critical feature to enable early plants to colonize the land and to support a plant's upright growth and defense (Popper and Fry 2003). Many plant–pathogenic microorganisms actively penetrate the plant apoplast in order to access intracellular nutrients. Cell wall structure and composition change during pathogenesis, partially due to microbial cell wall-degrading enzymes (CWDEs) secreted during pathogenesis (Laluk and Mengiste 2010), and partially due to plant-induced cell wall remodeling directed towards wall fortification (Hamann 2012; Underwood 2012). The hundreds of CWDEs secreted by pathogenic microbes into the plant apoplast vary depending on the microbe pathogen and the host species; these CWDEs are essential for successful pathogenesis (Kubicek et al. 2014).

In this constant battle with microorganisms, plants have developed a system for sensing pathogen penetration and other stresses. Plant Cell Wall Integrity (CWI) mechanisms rapidly remodel the cell wall in response to breaches of the wall or sensing fragmentation of the wall (Engelsdorf and Hamann 2014; Hamann and Denness 2011; Voxeur and Hofte 2016). During pathogenesis, plants perceive wall fragmentation by sensing wall-derived molecules produced by damage from microbial CWDEs. These damage-associated molecular patterns (DAMPs) together with microbe-associated molecular patterns (MAMPs) are recognized by membrane-bound pattern recognition receptors (PRR). The result is the induction of defense responses, including changes in signaling, transcriptional reprogramming, synthesis of defense metabolites, and cell wall remodeling (Boller and He 2009; Ferrari et al. 2013). For example, oligogalacturonide DAMPs are sensed by receptor Wall Associated Kinases 1 and 2 (WAK1, 2) (Brutus et al. 2010; Kohorn et al. 2014, 2016). WAKs are critical in promoting cell expansion in normal unstressed conditions (Wagner and Kohorn 2001), monitoring the pectin integrity disturbed during injury (De Lorenzo et al. 2011), and are involved in plant immune responses (Ferrari et al. 2013; Kohorn 2016). Similarly, several *Catharanthus roseus*-like RLKs (CrRLKs) monitor CWI and regulate growth in Arabidopsis: THESEUS1 (THE1), FERONIA (FER), and HERCULES1 (HERK1) sense structural defects in the cell wall, regulate cell expansion, and are integrated into the brassinosteroid signaling pathway (Hématy et al. 2007; Tang et al. 2008; Guo et al. 2009).

After PRRs sense changes in the apoplast, multiple signaling pathways transmit the signal to the nucleus to induce compensatory gene expression (Rodicio and Heinisch 2010). The signaling pathways involved are complex and not yet fully understood, perhaps due to their partially overlapping nature and sensitivity to common secondary messengers such as $Ca^{2+}$, ROS production, and inositol triphosphate (Godfrey and Rathjen 2012; Ma et al. 2012). In spite of this, some downstream responses are well characterized. FLAGELLIN-SENSING 2 (FLS2) and its co-receptor BRI-1 ASSOCIATED KINASE 1 bind extracellular bacterial flagellin, and initiate a mitogen-activated protein kinase (MPK) cascade, which in turn changes expression of a variety of gene targets (Asai et al. 2002; Navarro et al. 2004). WAKs, depending on their extracellular binding partner, phosphorylate proteins involved in signaling, activate MPK signaling pathways, and ultimately upregulate expression of defense response genes (Wagner and Kohorn 2001; Kohorn et al. 2014, 2016; Kohorn 2016). WAK1 also negatively regulates defense responses by forming complexes with the apoplast-localized glycine-rich protein GRP3, and cytoplasm-localized protein phosphatase (KAPP) (Gramegna et al. 2016).

The first evidence for CWI control mechanisms in plants was deduced from the physiology of mutants and pharmacological inhibition of cell wall biosynthetic processes (Hématy et al. 2007; Hamann et al. 2009; Ringli 2010; Wolf et al. 2012). Recently, a different approach for perturbation of the cell wall has been proposed: the post-synthetic modification of cell walls by overexpressing CWDEs targeted to the plant apoplast. This perturbation occurs directly *in muro* and thus can potentially more closely mimic the action of CWDEs secreted by microorganisms during pathogenesis (Pogorelko et al. 2013; Bellincampi et al. 2014; Lionetti et al. 2014). Induced post-synthetic modification of the cell wall through overexpression of CWDEs allows for two extracellular sensing mechanisms: the direct sensing of DAMPS liberated from the cell wall (Savatin et al. 2014), and the direct sensing of the microbial enzyme itself, which can be perceived as a MAMP (Wu et al. 2014). Both DAMPs and MAMPs are sensed by RLKs to induce Pattern-Triggered Immunity (PTI), the initial plant response for broad, nonspecific defense when challenged with a pathogen (Wu et al. 2014). Post-synthetic modification isolates the action of a single CWDE, and facilitates determination of signaling pathways activated by a specific M/DAMP.

Whole-transcriptome sequencing, known commonly as RNA-Seq, and microarray technology have become important tools for discovering novel signaling pathways and their components induced in response to environmental stresses (Guo et al. 2009; de Jonge et al. 2012; Rasmussen et al. 2013). Several studies have successfully used RNA-Seq to determine genes involved in CWI control and response to pathogens (Ehlting et al. 2008; De Cremer et al. 2013; Shen et al. 2014; Nafisi et al. 2015; Xu et al. 2017; Tsai et al. 2017). More recently, RNA-Seq has been used in combination with global metabolomics or proteomics analyses where a systems biology approach has been applied for correlative analyses to increase the power of predictions (Strauch et al. 2015; Li et al. 2015; Liu et al. 2016).

In this study, we combined the power of transcriptomics and metabolomics with the specificity provided by post-synthetic modification. We examined the transcriptome and metabolome of three transgenic CWDE-expressing Arabidopsis lines and compared them with control plants overexpressing green fluorescent protein in an empty vector (EV). The CWDE-expressing plants include two previously characterized acetylesterase-expressing lines: *Aspergillus nidulans*-derived acetylxylanesterase (AnAXE) and rhamnogalacturonan acetylesterase (AnRAE), which exhibit increased defense responses and reduced susceptibility to *Botrytis cinerea* (Pogorelko et al. 2013). We selected a third line expressing an *A. nidulans* ferulic acid esterase (AnFAE), previously shown to have increased susceptibility to *B. cinerea* (Reem et al. 2016). Transcriptome and metabolome datasets were correlated to determine the metabolic pathways most likely involved in the differential defense responses seen in AnAXE, AnRAE, and AnFAE lines relative to the control EV plants.

## Materials and methods

### Plant materials and growth conditions

*Arabidopsis* seeds (ecotype Columbia-0) were sterilized with 70% ethanol and 0.5% bleach, washed with sterile water, and planted on petri plates containing 1/2-strength Murashige and Skoog (1962) medium containing 2% sucrose and 0.3% Gelrite (Research Products International, Mt. Prospect, IL, USA). Plants were grown for 14 days in a growth chamber under the following conditions: 16-h light/ 8-h dark at 21 °C and 65% relative humidity, and light intensity of 160 µmol $s^{-1}$ $m^{-2}$. Plates with different transgenic lines and control plants were randomly distributed on the shelf to minimize the potential effects of small differences in light and temperature. At the time of harvest, plants were cut at the base of the hypocotyl and the entire aboveground portion of all plants were immediately placed in a 50 mL conical tube immersed in liquid nitrogen, and stored at − 80 °C until analysis.

For RT-qPCR analyses, seeds were planted on autoclaved LC-1 potting soil mix (Sun Gro Horticulture, Agawam, MA, USA) and plants were grown in a growth chamber under 16-h light/8-h dark conditions at 21 °C, 65% relative humidity, and light intensity of 160 µmol $s^{-1}$ $m^{-2}$.

### Preparation of RNA and RNA-Seq

For RNA-Seq, 1 g of plant tissue was homogenized using RNase-free mortar and pestles, then transferred to tubes containing TRIZOL reagent (Invitrogen Life Technologies, CA, USA). RNA was extracted according to the manufacturer's protocol and solubilized in DEPC-treated water, then treated with DNase I for 30 min at 37 °C (Invitrogen Corp., Carlsbad, CA, USA). RNA was cleaned up using an RNEasy Mini Kit (Qiagen, CA, USA). Sixty micrograms of total RNA was provided for sequencing, which was performed by BGI Americas (http://www.BGI.com).

For RT-qPCR, RNA was extracted using the same method as above. One microgram of total RNA was reverse-transcribed to cDNA using SuperScript III First Strand Synthesis system (Invitrogen Corp., Carlsbad, CA, USA), then digested with RNase H to purify the cDNA.

### RNA-Seq analysis: counting and mapping reads, statistical analysis for DE genes

For RNA-Seq, total RNA from 20 seedlings was extracted for each biological replicate. Four biological replicates were analyzed for each transgenic line and control. Sequencing was conducted using an Illumina HiSeq 2000 system with 100-cycle paired-ends at BGI Americas (http://www.BGI.com). The cleaned reads were aligned to the reference genome of *Arabidopsis thaliana* using TopHat (Trapnell et al. 2009), and the mapped reads were counted using htseq-count (http://www-huber.embl.de/users/anders/HTSeq/doc/count.html). Genes were tested for differential expression (DE) using the negative binomial QLShrink (Lund et al. 2012) and the R package QuasiSeq (http://cran.r-project.org/web/packages/QuasiSeq).

### RT-qPCR

Gene expression was conducted using cDNA from four biological replicates, with two technical replicates each. Expression was quantified using the Maxima SYBR Green qPCR Master Mix (Invitrogen Corp) and the CFX-96 Thermal Cycler (Bio-Rad) using primers appropriate for each gene (Supplementary Table 5). Relative expression levels were calculated using the comparative threshold cycle method (Schmittgen and Livak 2008), in which gene expression levels of wild-type plants were normalized to 1 and expression of transgenic lines was calculated relative to this level.

### Metabolite extraction and LC/MS analysis

Metabolites were extracted from the same plants used from RNAseq analysis. 100 mg of plant tissue was finely ground with mortar and pestle, then incubated in 50% (v/v) methanol at 65 °C for 40 min. Samples were centrifuged at 16,000×*g* for 5 min and passed through a 0.2 µm regenerated cellulose filter.

Untargeted metabolite profiling was carried out on an Agilent G6530A Q-TOF LC/MS system. Ten microliters of metabolite extract was injected onto an Agilent Eclipse

Plus C18 column (3 × 100 mm; 1.8 µm). Metabolites were separated using a binary gradient of solvent A (0.1% formic acid in water) and solvent B (0.1% formic acid in acetonitrile) at a flow rate of 0.6 mL $min^{-1}$. The gradient starts at 2% solvent B for 1 min, followed by a linear increase to 98% over 20 min. The acquisition of mass spectra was done in negative mode with the following parameters: drying gas temperature, 300 °C; drying gas flow rate, 7.0 L $min^{-1}$; nebulizer pressure, 40 psi; sheath gas temperature, 350 °C; sheath gas flow rate, 10.0 L $min^{-1}$; Vcap, 3500 V; Nozzle Voltage, 500 V; Fragmentor, 150 V; Skimmer, 65 V; Octopole RF Peak, 750 V.

The raw data were processed using Agilent Masshunter Profinder (Version B.06.00) to extract mass peaks and align them across all the samples. The output files were imported into Agilent Mass Profiler Professional (Version B.13.11) for statistical analysis. Hierarchical clustering analysis was performed on $\log_2$ transformed and normalized data using Euclidean distance and Ward's linkage rule.

Metabolites were annotated by searching the accurate mass against KNApSAcK (http://kanaya.naist.jp/KNApSAcK/) and PlantCyc (https://www.plantcyc.org/) databases. The relative mass difference of 10 ppm was used as a cutoff for database search. The peaks were first searched against the Arabidopsis metabolites (*A. thaliana* in KNApSAcK and AraCyc, designated as At database in Supplementary Table 3), resulting in annotation of 63 peaks. The unmatched peaks were then searched against all plant metabolites in the KNApSAcK and PlantCyc databases (designated as Pl database in Supplementary Table 3). Together, 235 peaks were annotated.

### Transcript-metabolite correlation

The entire raw transcriptome dataset, represented as Fragments Per Kilobase of transcript per Million mapped reads (FPKM), and the entire metabolome dataset, formatted in $\log_2$ abundance (peak area), along with their metadata, were uploaded to the Plant/eukaryotic and Microbial Systems Resource (PMR) database (PMR: http://www.metnetdb.org/pmr) (Hur et al. 2013).

Statistical significance of metabolite abundances was calculated through the PMR database by comparing the metabolite abundances of hydrolase-expressing line (AnAXE, AnRAE, AnFAE) with the EV control. Metabolites with q-values less than 0.1 were considered for further correlation analysis. For each metabolite, lists of genes were identified according to metabolite-transcript correlation (Pearson correlation coefficient > 0.9). Genes meeting this cutoff were then used to determine over-represented pathways through MetNetOnline (http://www.metnetonline.org). From the resultant enriched gene list, significantly enriched pathways ($p < 0.05$) were determined for every metabolite, and then pooled together. The individual pathways and their relevant locus IDs were then ranked according to the number of metabolites associated with them. This yielded a final list of enriched pathways for each transgenic line, ranked according to occurrence along with their relevant gene expressions (Table 4).

## Results

### Differentially expressed genes in transgenic plants expressing wall-modifying hydrolases

Total RNA was sequenced from rosettes of 2-week old AnAXE, AnRAE, AnFAE, and EV control lines. Expression data were analyzed with the quasiSeq R package to yield p- and q-values for each transcript. A histogram of p-values was first checked to estimate number of true null hypotheses (Nettleton et al. 2006). The resulting distribution was approximately flat, resulting in high q-values in all comparisons (Supplementary Figure 1). A comparison of AnFAE and EV samples showed six genes with q-values less than 0.2 (AT1G20160, AT1G50110, AT3G50630, AT3G54960, AT4G00700, AT4G14420). No other comparisons between genotypes yielded q-values in this range.

Due to high q-values in this dataset, the Differentially Expressed (DE) genes were determined using a p-value threshold of less than 0.05 and greater than twofold difference in expression between samples. Using this method of analysis, it is important to acknowledge the likelihood of false positives present in this gene list, since there is no correction for multiple testing. However, since this dataset was used later for correlation analysis, and also contains true positives, we proceeded with a general analysis of the transcriptome in an attempt to obtain candidate genes. We identified DE genes between CWDE-expressing and EV control plants. Fifty-nine genes were upregulated more than twofold ($p < 0.05$) in AnAXE, 60 genes in AnRAE, and 79 genes in AnFAE in comparison with the EV plants. One hundred genes were downregulated more than twofold ($p < 0.05$) in AnAXE, 127 genes in AnRAE, and 409 genes in AnFAE in comparison with the EV plants (Fig. 1a). Most of the DE genes were unique to a particular transgenic line. The Venny online tool (http://bioinfogp.cnb.csic.es/tools/venny) was used to determine overlapping DE genes between the three transgenic lines. A relatively small proportion of genes were commonly up- or down-regulated between the three CWDE-expressing lines, and no Gene Ontology (GO) enrichment was found using the Panther Gene Ontology Tool (Fig. 1). The entire transcriptome dataset is presented in Supplementary Table 1, and is also available in the Plant/Eukaryotic and Microbial Systems Resource (PMR; http://metnetdb.

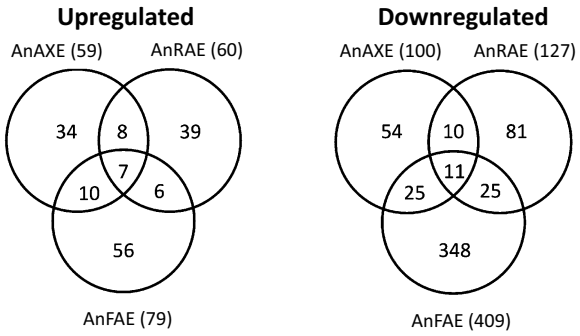


**Fig. 1** DE genes from RNAsEq. Venn diagrams showing upregulated (left) and downregulated (right) genes relative to EV control. Values in parentheses indicate total number of DE genes

org/pmr) (Hur et al. 2013). All DE genes are shown in Supplementary Table 2.

## Stress response, cell wall remodeling, and transcription factor enrichments in transcriptome

To better understand the response of each transgenic line to cell wall modification, molecular functions and protein classes enriched in DE genes were determined using the Panther GO enrichment tool. Upregulated genes with known functions encode nucleic acid binding proteins, transporters, hydrolases, and receptors (Supplementary Figure 2). Significant numbers of downregulated genes also encode nucleic acid binding proteins, transporters, and hydrolases, as well as oxidoreductases and transferases (Supplementary Figure 2). In order to further investigate the plant responses induced by these CW modifications or by the overexpressed CWDEs, the DE genes were sorted according to known association with cell wall modification, stress response, and transcriptional regulation (Tables 1, 2, 3). DE genes in each table are shown in bold, and uniquely up- or down-regulated genes are underlined.

Of genes related to cell wall processes, the AnAXE plants upregulated three genes, two of which were unique (not upregulated in another line): Cellulase 3 and Purple Acid Phosphatase 25 (Table 1). 16 genes were downregulated in AnAXE, 2 of which were unique: Peroxidase 52 and Expansin A21 (Table 1). AnRAE plants only upregulated 1 gene, Plant Defensin 1.2b, which was also upregulated in AnFAE plants. 18 genes were downregulated in AnRAE plants, and 2 of them were unique: one uncharacterized gene and Cellulose Synthase-Like C12 (Table 1). AnFAE plants upregulated 9 wall-related genes, 6 of which were unique, including Plant Defensin 1.2 and Plant Defensin 1.3, and xyloglucan endotransglycosylases 6 and 18 (Table 1). 48 genes were downregulated in AnFAE plants, 27 of which were unique genes that include xyloglucan endotransglycosylases 13 and 14 and Reduced Wall Phenolics 1, a feruloyl transferase (Table 1).

DE genes related to stress response showed 7 plants upregulated in AnAXE plants, with 3 unique genes including Chitinase A (Table 2). 18 genes were downregulated in AnAXE, 6 of which were unique, including Wall Associated Kinase-Like 10, Cys-rich RLK 13 and 30, and Mildew Resistance Locus O 15 (Table 2). AnRAE plants upregulated 5 genes, of which 3 were unique, including PDF1.4 and CYP81G1. 12 genes were downregulated in AnRAE, but only 2 were unique; both are uncharacterized genes (Table 2). AnFAE plants upregulated 15 genes, 10 of which were unique, including JAZ5, 7, and 10, and MYB47. 59 genes were downregulated in AnFAE plants, and 39 of these were unique. This includes a large number of uncharacterized genes, as well as FLG22-Induced Receptor-Like Kinase 1, Cys-Rich RLK 36, and WRKY27 (Table 2).

Analysis of transcriptional regulators revealed AnAXE plants upregulated 8 genes; 2 of these were unique to AnAXE, but both are uncharacterized. 14 genes were downregulated in AnAXE, 5 of which were unique, including WRKY30 and MYB66 (Table 3). AnRAE plants upregulated 8 genes, and 2 were unique. 20 genes were downregulated in AnRAE, including 8 unique genes (Table 3). AnFAE plants upregulated 13 transcriptional regulators, 7 of which were unique, including the previously mentioned JAZ proteins. 42 genes were downregulated in AnFAE, with 24 unique genes, including WRKY61, MYB63, and MYB68 (Table 3).

## Mapping stress responses in plants

To assist in identifying responses to cell wall modifications in the mutants, MapMan software was used to map gene expression associated with stress among the DE genes (Fig. 2). Mapping gene expression in AnAXE revealed a large number of DE genes involved in signaling and proteolysis. In addition, upregulation of WRKY transcription factors, and downregulation of MYB transcription factors was observed in AnAXE plants. Noticeable gene expression changes in plant hormone signaling were also observed, including mixed expression in auxin signaling, and upregulation of ethylene signaling (Fig. 2a). Like AnAXE, the AnRAE plants also possessed a large number of DE genes involved in signaling and proteolysis, as well as cell wall metabolism. WRKY and MYB transcription factors showed similar expression patterns to those observed in the AnAXE plants. Hormone signaling, however, was different in AnRAE plants; auxin and ethylene signaling were largely downregulated (Fig. 2b). As expected, fewer similarities were found in the AnFAE plants in comparison with AnRAE and AnAXE. While signaling, proteolysis, and cell

**Table 1** Cell wall-related DE genes in AnAXE, AnRAE, and AnFAE plants

| Gene | Name | Description | $Log_2$-fold change | | |
|---|---|---|---|---|---|
| | | | AnAXE-EV | AnRAE-EV | AnFAE-EV |
| AT1G02360 | AT1G02360 | | −0.62 | −0.41 | **−1.22** |
| AT1G02460 | AT1G02460 | | **−1.06** | **−1.69** | −0.55 |
| AT1G04980 | PDIL2-2 | PDI-like 2-2 | **−1.29** | **−1.40** | **−1.16** |
| AT1G05260 | RCI3 | RARE COLD INDUCIBLE GENE 3 | −0.35 | −0.71 | **−1.36** |
| AT1G08990 | PGSIP5 | Plant glycogenin-like starch initiation protein 5 | −0.20 | −0.48 | **−1.84** |
| AT1G12040 | LRX1 | Leucine-rich repeat/extensin 1 | −0.80 | −0.95 | **−2.33** |
| AT1G20150 | AT1G20150 | | 0.43 | **−1.87** | **1.79** |
| AT1G21310 | EXT3 | Extensin 3 | −0.59 | −0.26 | **−1.15** |
| AT1G23720 | AT1G23720 | | **−1.13** | −0.68 | **−2.46** |
| AT1G35140 | PHI-1 | PHOSPHATE-INDUCED 1 | 0.20 | −0.30 | **1.14** |
| AT1G44130 | AT1G44130 | | −0.83 | −0.33 | **−2.18** |
| AT1G48930 | GH9C1 | Glycosyl hydrolase 9C1 | −0.90 | **−1.52** | **−2.37** |
| AT1G54970 | PRP1 | Proline-rich protein 1 | −0.99 | **−1.18** | **−2.73** |
| AT1G65610 | KOR2 | KORRIGAN 2 | −0.82 | −0.71 | **−1.63** |
| AT1G71380 | CEL3 | Cellulase 3 | **1.19** | 0.62 | −0.06 |
| AT1G73410 | MYB54 | myb domain protein 54 | 0.09 | **−1.22** | **−1.00** |
| AT1G78860 | AT1G78860 | | −0.95 | **−1.45** | −0.66 |
| AT1G79180 | MYB63 | myb domain protein 63 | −0.32 | −0.47 | **−1.71** |
| AT1G80240 | DGR1 | DUF642 L-GalL responsive gene 1 | −0.38 | −0.64 | **−1.12** |
| AT2G18150 | AT2G18150 | | −0.48 | −0.75 | **−1.08** |
| AT2G24980 | EXT6 | Extensin 6 | **−1.24** | **−1.07** | **−2.69** |
| AT2G26010 | PDF1.3 | Plant defensin 1.3 | 0.27 | 0.43 | **2.46** |
| AT2G26020 | PDF1.2b | Plant defensin 1.2b | 0.76 | **1.19** | **2.33** |
| AT2G27370 | CASP3 | Casparian strip membrane domain protein 3 | **−1.22** | **−1.55** | **−2.59** |
| AT2G33790 | AGP30 | Arabinogalactan protein 30 | −0.52 | −0.28 | **−2.56** |
| AT2G36100 | CASP1 | Casparian strip membrane domain protein 1 | −0.83 | −0.37 | **−2.49** |
| AT2G38380 | AT2G38380 | | −0.54 | −0.75 | **−1.31** |
| AT2G45220 | AT2G45220 | | −0.63 | −0.19 | **−1.02** |
| AT2G46740 | GulLO5 | L-Gulono-1,4-lactone (L-GulL) oxidase 5 | −0.16 | −0.95 | **−2.18** |
| AT3G11550 | CASP2 | Casparian strip membrane domain protein 2 | −0.37 | −0.01 | **−1.10** |
| AT3G28550 | AT3G28550 | | **−1.29** | −0.89 | **−2.73** |
| AT3G52790 | AT3G52790 | | −0.69 | −0.49 | **−2.01** |
| AT3G54580 | AT3G54580 | | **−1.25** | −0.82 | **−2.94** |
| AT3G62680 | PRP3 | Proline-rich protein 3 | −0.82 | −0.81 | **−2.71** |
| AT4G01630 | EXPA17 | Expansin A17 | −0.57 | **−1.77** | **−1.12** |
| AT4G07960 | CSLC12 | Cellulose-synthase-like C12 | 0.12 | **−1.11** | 0.07 |
| AT4G08400 | AT4G08400 | | −0.68 | **−1.05** | **−2.76** |
| AT4G08410 | AT4G08410 | | **−1.14** | −0.96 | **−2.58** |
| AT4G11050 | GH9C3 | Glycosyl hydrolase 9C3 | **2.13** | 0.89 | **1.68** |
| AT4G13390 | EXT12 | Extensin 12 | **−1.08** | −0.78 | **−2.74** |
| AT4G25810 | XTR6 | Xyloglucan endotransglycosylase 6 | 0.12 | −0.30 | **1.19** |
| AT4G25820 | XTH14 | Xyloglucan endotransglucosylase/hydrolase 14 | −0.82 | −0.84 | **−2.33** |
| AT4G28850 | XTH26 | Xyloglucan endotransglucosylase/hydrolase 26 | **−1.52** | **−2.00** | **−3.68** |
| AT4G30280 | XTH18 | Xyloglucan endotransglucosylase/hydrolase 18 | 0.44 | −0.72 | **1.02** |
| AT4G36350 | PAP25 | Purple acid phosphatase 25 | **1.13** | −0.12 | 0.49 |
| AT4G36430 | AT4G36430 | | −0.32 | −0.83 | **−1.02** |
| AT4G37160 | sks15 | SKU5 similar 15 | −0.41 | −0.45 | **−2.49** |
| AT5G04960 | AT5G04960 | | −0.79 | **−1.05** | **−2.15** |

**Table 1** (continued)

| Gene | Name | Description | $Log_2$-fold change | | |
|---|---|---|---|---|---|
| | | | AnAXE-EV | AnRAE-EV | AnFAE-EV |
| AT5G05340 | PRX52 | Peroxidase 52 | **−1.29** | −0.87 | −0.92 |
| AT5G06630 | AT5G06630 | | **−1.46** | **−1.25** | **−2.65** |
| AT5G06640 | EXT10 | Extensin 10 | **−1.07** | −0.68 | **−2.40** |
| AT5G08150 | SOB5 | SUPPRESSOR OF PHYTOCHROME B 5 | 0.23 | 0.25 | **1.20** |
| AT5G11920 | cwINV6 | 6-&1-Fructan exohydrolase | −0.65 | −0.05 | **−1.47** |
| AT5G15290 | CASP5 | Casparian strip membrane domain protein 5 | −0.51 | **−1.90** | **−3.08** |
| AT5G17820 | AT5G17820 | | −0.81 | **−1.01** | **−1.95** |
| AT5G22410 | RHS18 | Root hair specific 18 | **−1.07** | −0.63 | **−2.08** |
| AT5G35190 | EXT13 | Extensin 13 | **−1.01** | −0.66 | **−2.70** |
| AT5G39260 | EXPA21 | Expansin A21 | **−1.19** | −0.02 | −0.88 |
| AT5G41040 | RWP1 | REDUCED LEVELS OF WALL-BOUND PHENOLICS 1 | −0.35 | −0.79 | **−1.18** |
| AT5G42020 | BIP2 | | −0.93 | **−1.07** | **−1.03** |
| AT5G44420 | PDF1.2 | Plant defensin 1.2 | −0.57 | −0.22 | **1.49** |
| AT5G57540 | XTH13 | Xyloglucan endotransglucosylase/hydrolase 13 | −0.63 | −0.65 | **−3.72** |
| AT5G59090 | SBT4.12 | Subtilase 4.12 | −0.62 | −0.34 | **−2.07** |
| AT5G64100 | AT5G64100 | | −0.83 | −0.40 | **−2.07** |

Values in bold represent significantly different gene expression relative to EV plants ($p < 0.05$). Underlined values indicate unique up- or down-regulation

wall metabolism were also among the most highly enriched stress responses, the AnFAE plants exhibited downregulation of MYB transcription factors, and increased expression of ethylene response factors (ERF). In addition, the AnFAE plants showed downregulation of genes encoding peroxidases (Fig. 2c).

Heat map analysis of all DE genes highlights the similarities between AnAXE and AnRAE, as well as their differences with AnFAE (Fig. 2d). While the expression pattern of cell wall-related genes was similar between AnAXE and AnRAE plants, with only a small number of genes downregulated, a large number of cell wall-related genes were downregulated in the AnFAE plants. In addition, significant downregulation of genes involved in lipid metabolism was found in AnFAE plants. A larger number of signaling-related genes were differentially expressed in AnFAE plants in comparison with AnAXE and AnRAE plants. Some variations were observed among all three lines in DE genes related to stress response, secondary metabolism, and hormone metabolism (Fig. 2d).

## Confirmation of gene expression through RT-qPCR

Real-Time Quantitative PCR (RT-qPCR) was used to confirm RNA-Seq results. A set of separately grown transgenic plants was used for these analyses. The genes were selected for RT-qPCR based on expression levels; some were classified as DE genes, and some were not differentially expressed (Fig. 3). Expression of MLO12 was confirmed to be downregulated in AnAXE and AnFAE. Upregulation of JAZ5 was observed in AnFAE, and CAD2 expression in AnFAE plants remained slightly upregulated relative to EV, whereas no change was detected in AnAXE or AnRAE. Upregulation of WRKY40 was observed in AnAXE plants, and no change was detected in expression of ICS1 or CYP94C1. AnRAE plants also exhibited upregulation of MPK14, and downregulation of ACS2, ICS1, and CYP71A13 (Fig. 3).

## Metabolome analysis of transgenic plants

Untargeted metabolomic analysis was used to characterize the global metabolome changes in AnAXE, AnRAE, and AnFAE plants in comparison with the EV plants. Total metabolites were extracted from the same plant tissues used for transcriptome analysis, and were analyzed using LC/MS. In total, 482 metabolites were detected; 235 of these were annotated. Some of these metabolites accumulated to levels significantly different in comparison with the EV plants in at least one line. In AnAXE plants, 46 metabolites were more abundant and 18 were less abundant in comparison with EV. AnRAE plants possessed 26 more abundant and 18 less abundant metabolites. In AnFAE plants, 26 metabolites were more abundant and 13 were less abundant (Fig. 4a). All detected metabolites and their abundance are presented in Supplementary Table 3, and are also available through the PMR database.

**Table 2** DE stress and defense response genes in AnAXE, AnRAE, and AnFAE plants

| Gene | Name | Description | $Log_2$-fold change | | |
|---|---|---|---|---|---|
| | | | AnAXE-EV | AnRAE-EV | AnFAE-EV |
| AT1G02360 | AT1G02360 | | −0.62 | −0.41 | **−1.22** |
| AT1G04980 | PDIL2-2 | PDI-like 2-2 | **−1.29** | **−1.40** | **−1.16** |
| AT1G05260 | RCI3 | RARE COLD INDUCIBLE GENE 3 | −0.35 | −0.71 | **−1.36** |
| AT1G09090 | RBOHB | Respiratory burst oxidase homolog B | −0.28 | −0.47 | **−1.61** |
| AT1G17380 | JAZ5 | Jasmonate-zim-domain protein 5 | 0.53 | 0.01 | **1.16** |
| AT1G18710 | MYB47 | myb domain protein 47 | 0.88 | 0.45 | **1.02** |
| AT1G19610 | PDF1.4 | | 0.69 | **1.12** | 0.41 |
| AT1G30870 | AT1G30870 | | −0.40 | **−1.10** | **−2.12** |
| AT1G34510 | AT1G34510 | | −0.30 | −0.53 | **−4.30** |
| AT1G49570 | AT1G49570 | | **−1.82** | −0.98 | **−2.24** |
| AT1G51800 | IOS1 | IMPAIRED OOMYCETE SUSCEPTIBILITY 1 | **−1.13** | −0.82 | **−1.41** |
| AT1G58170 | AT1G58170 | | 0.08 | −0.65 | **−1.03** |
| AT1G65690 | AT1G65690 | | −0.25 | −0.42 | **−1.03** |
| AT1G66270 | BGLU21 | | −0.33 | −0.52 | **−1.76** |
| AT1G66280 | BGLU22 | | −0.23 | −0.58 | **−1.94** |
| AT1G68850 | AT1G68850 | | −0.28 | −0.58 | **−1.77** |
| AT1G77120 | ADH1 | Alcohol dehydrogenase 1 | **−1.02** | −0.59 | **−1.38** |
| AT1G79680 | WAKL10 | WALL ASSOCIATED KINASE (WAK)-LIKE 10 | **−1.04** | −0.50 | −0.78 |
| AT2G01520 | MLP328 | MLP-like protein 328 | −0.31 | −0.52 | **−1.57** |
| AT2G18150 | AT2G18150 | | −0.48 | −0.75 | **−1.08** |
| AT2G18980 | AT2G18980 | | −0.87 | −0.95 | **−1.46** |
| AT2G19190 | FRK1 | FLG22-induced receptor-like kinase 1 | −0.92 | 0.23 | **−1.24** |
| AT2G19590 | ACO1 | ACC oxidase 1 | −0.80 | −0.58 | **−1.08** |
| AT2G21100 | AT2G21100 | | −0.16 | **−1.25** | **−1.39** |
| AT2G26010 | PDF1.3 | Plant defensin 1.3 | 0.27 | 0.43 | **2.46** |
| AT2G26020 | PDF1.2b | Plant defensin 1.2b | 0.76 | **1.19** | **2.33** |
| AT2G34600 | JAZ7 | Jasmonate-zim-domain protein 7 | 0.29 | 0.03 | **1.45** |
| AT2G35000 | ATL9 | Arabidopsis toxicos en levadura 9 | −0.57 | −1.00 | **−1.65** |
| AT2G35380 | AT2G35380 | | −0.72 | −0.86 | **−1.70** |
| AT2G38380 | AT2G38380 | | −0.54 | −0.75 | **−1.31** |
| AT2G39200 | MLO12 | MILDEW RESISTANCE LOCUS O 12 | **−1.47** | −0.65 | −0.70 |
| AT2G42885 | AT2G42885 | | −0.07 | 0.09 | **1.89** |
| AT2G44110 | MLO15 | MILDEW RESISTANCE LOCUS O 15 | −0.25 | −0.70 | **−2.39** |
| AT2G45220 | AT2G45220 | | −0.63 | −0.19 | **−1.02** |
| AT2G47770 | TSPO | TSPO (outer membrane tryptophan-rich sensory protein)-related | **1.85** | **1.09** | **1.52** |
| AT2G48150 | GPX4 | Glutathione peroxidase 4 | −0.32 | **−2.20** | **−3.17** |
| AT3G01190 | AT3G01190 | | **−1.10** | −0.45 | **−1.90** |
| AT3G04570 | AHL19 | AT-hook motif nuclear-localized protein 19 | −0.35 | −0.46 | **−1.40** |
| AT3G09940 | MDHAR | Monodehydroascorbate reductase | −0.78 | −0.73 | **−1.60** |
| AT3G11340 | UGT76B1 | UDP-dependent glycosyltransferase 76B1 | −0.86 | −0.34 | **−1.73** |
| AT3G20340 | AT3G20340 | | 0.56 | **1.47** | −0.27 |
| AT3G22275 | AT3G22275 | | 0.76 | 0.81 | **1.97** |
| AT3G25510 | AT3G25510 | | −0.61 | −0.35 | **−1.28** |
| AT3G25930 | AT3G25930 | | −0.39 | 0.07 | **−2.10** |
| AT3G28740 | CYP81D11 | Cytochrome P450, family 81, subfamily D, polypeptide 11 | 0.93 | 0.70 | **1.08** |
| AT3G49960 | AT3G49960 | | −0.36 | **−1.23** | **−2.50** |
| AT3G55230 | AT3G55230 | | −0.33 | −0.27 | **−1.58** |
| AT3G60120 | BGLU27 | Beta glucosidase 27 | **−2.55** | **−1.37** | **−1.88** |

**Table 2** (continued)

| Gene | Name | Description | $Log_2$-fold change | | |
|---|---|---|---|---|---|
| | | | AnAXE-EV | AnRAE-EV | AnFAE-EV |
| AT4G04490 | CRK36 | Cysteine-rich RLK (RECEPTOR-like protein kinase) 36 | −0.30 | −0.51 | **−1.04** |
| AT4G04500 | CRK37 | Cysteine-rich RLK (RECEPTOR-like protein kinase) 37 | −0.81 | −0.62 | **−1.30** |
| AT4G10500 | AT4G10500 | | −0.69 | −0.57 | **−1.32** |
| AT4G11170 | AT4G11170 | | **−1.16** | −0.65 | **−2.85** |
| AT4G11460 | CRK30 | Cysteine-rich RLK (RECEPTOR-like protein kinase) 30 | **−1.66** | −0.06 | −0.59 |
| AT4G19030 | NLM1 | NOD26-like major intrinsic protein 1 | −0.18 | −0.08 | **−2.69** |
| AT4G21440 | MYB102 | MYB-like 102 | **1.14** | −0.06 | **1.18** |
| AT4G23200 | CRK12 | Cysteine-rich RLK (RECEPTOR-like protein kinase) 12 | **−1.08** | −0.84 | **−1.09** |
| AT4G23210 | CRK13 | Cysteine-rich RLK (RECEPTOR-like protein kinase) 13 | **−1.34** | 0.33 | −0.05 |
| AT4G26010 | AT4G26010 | | −0.92 | −0.76 | **−2.31** |
| AT4G30170 | AT4G30170 | | −0.56 | −0.13 | **−1.80** |
| AT4G33730 | AT4G33730 | | −0.59 | −0.70 | **−3.67** |
| AT4G36430 | AT4G36430 | | −0.32 | −0.83 | **−1.02** |
| AT4G37070 | PLP1 | | −0.27 | −0.54 | **−1.99** |
| AT5G01900 | WRKY62 | WRKY DNA-binding protein 62 | **−1.09** | −0.99 | **−1.00** |
| AT5G03210 | DIP2 | DBP-interacting protein 2 | **1.73** | −0.80 | −0.57 |
| AT5G05340 | PRX52 | Peroxidase 52 | **−1.29** | −0.87 | −0.92 |
| AT5G06760 | LEA4-5 | Late embryogenesis abundant 4-5 | **1.55** | 0.33 | **1.14** |
| AT5G13220 | JAZ10 | Jasmonate-zim-domain protein 10 | 0.44 | −0.28 | **1.41** |
| AT5G16980 | AT5G16980 | | **1.05** | 0.56 | 0.69 |
| AT5G17390 | AT5G17390 | | −0.88 | **−3.27** | −0.94 |
| AT5G17820 | AT5G17820 | | −0.81 | **−1.01** | **−1.95** |
| AT5G22410 | RHS18 | Root hair specific 18 | **−1.07** | −0.63 | **−2.08** |
| AT5G24090 | CHIA | Chitinase A | **1.08** | 0.51 | 0.06 |
| AT5G25370 | PLDALPHA3 | Phospholipase D alpha 3 | −0.05 | −0.32 | **−1.11** |
| AT5G28510 | BGLU24 | Beta glucosidase 24 | −0.52 | **−3.44** | **−2.07** |
| AT5G38000 | AT5G38000 | | −0.34 | **−1.12** | −0.82 |
| AT5G38340 | AT5G38340 | | **−1.05** | −0.49 | **−1.28** |
| AT5G42020 | BIP2 | | −0.93 | **−1.07** | **−1.03** |
| AT5G44420 | PDF1.2 | Plant defensin 1.2 | −0.57 | −0.22 | **1.49** |
| AT5G44610 | MAP18 | Microtubule-associated protein 18 | −0.73 | **−1.02** | **−1.98** |
| AT5G45220 | AT5G45220 | | **−1.93** | −0.01 | −0.72 |
| AT5G51060 | RHD2 | ROOT HAIR DEFECTIVE 2 | **−1.07** | −0.84 | **−1.38** |
| AT5G52300 | LTI65 | LOW-TEMPERATURE-INDUCED 65 | **1.37** | 0.29 | **1.06** |
| AT5G52830 | WRKY27 | WRKY DNA-binding protein 27 | −0.71 | −0.28 | **−1.50** |
| AT5G58400 | AT5G58400 | | 0.00 | 0.63 | **1.36** |
| AT5G64100 | AT5G64100 | | −0.83 | −0.40 | **−2.07** |
| AT5G66390 | AT5G66390 | | −0.28 | −0.55 | **−2.05** |
| AT5G67310 | CYP81G1 | Cytochrome P450, family 81, subfamily G, polypeptide 1 | 0.60 | **1.33** | 0.91 |
| AT5G67400 | RHS19 | Root hair specific 19 | −0.75 | −0.84 | **−2.16** |

Bold values indicate significantly different expression from EV plants ($p < 0.05$). Underlined values indicate unique up- or down-regulation

Compared to the transcriptome analysis, in which most DE gene transcripts were unique to a given transgenic line, a large proportion of differentially accumulated metabolites overlapped between the transgenic lines. Among upregulated metabolites, more metabolites were common to all lines than were unique to any single line. In fact, AnRAE lines had no unique upregulated metabolites, while AnFAE had just 2. Downregulated metabolites showed a similar pattern, with more shared metabolites

**Table 3** DE transcription factors expressed in AnAXE, AnRAE, and AnFAE plants

| Gene | Name | Description | $Log_2$-fold change | | |
|---|---|---|---|---|---|
| | | | AnAXE-EV | AnRAE-EV | AnFAE-EV |
| AT1G09540 | MYB61 | myb domain protein 61 | −0.45 | **−1.45** | **−1.88** |
| AT1G13300 | HRS1 | HYPERSENSITIVITY TO LOW PI-ELICITED PRIMARY ROOT SHORTENING 1 | −0.98 | −0.69 | **−1.22** |
| AT1G14686 | AT1G14686 | | **1.80** | **1.59** | **1.34** |
| AT1G17380 | JAZ5 | Jasmonate-zim-domain protein 5 | 0.53 | 0.01 | **1.16** |
| AT1G18710 | MYB47 | myb domain protein 47 | 0.88 | 0.45 | **1.02** |
| AT1G18860 | WRKY61 | WRKY DNA-binding protein 61 | −0.44 | −0.96 | **−1.17** |
| AT1G19510 | RL5 | RAD-like 5 | **1.33** | **1.46** | **1.44** |
| AT1G26680 | AT1G26680 | | −0.56 | **−3.07** | **−1.14** |
| AT1G27720 | TAF4B | TBP-associated factor 4B | −0.51 | **−1.28** | −0.40 |
| AT1G29280 | WRKY65 | WRKY DNA-binding protein 65 | −0.41 | −0.36 | **−1.53** |
| AT1G33760 | AT1G33760 | | **1.03** | −0.23 | 0.92 |
| AT1G49900 | AT1G49900 | | −0.34 | −0.80 | **−1.59** |
| AT1G53690 | AT1G53690 | | **−1.92** | 0.07 | −0.98 |
| AT1G54840 | AT1G54840 | | **−1.26** | −0.19 | −0.47 |
| AT1G62490 | AT1G62490 | | 0.05 | **−2.15** | 0.20 |
| AT1G67260 | TCP1 | | −0.16 | −0.83 | **−2.67** |
| AT1G73410 | MYB54 | myb domain protein 54 | 0.09 | **−1.22** | **−1.00** |
| AT1G74890 | ARR15 | Response regulator 15 | **−1.43** | −0.17 | 0.22 |
| AT1G79180 | MYB63 | myb domain protein 63 | −0.32 | −0.47 | **−1.71** |
| AT2G04038 | bZIP48 | Basic leucine-zipper 48 | **3.09** | **2.56** | **2.64** |
| AT2G20080 | AT2G20080 | | **−1.74** | **−1.15** | **−2.09** |
| AT2G21650 | MEE3 | MATERNAL EFFECT EMBRYO ARREST 3 | **−1.60** | −0.82 | **−1.53** |
| AT2G28160 | FRU | FER-like regulator of iron uptake | −0.37 | **−1.16** | −0.40 |
| AT2G28610 | PRS | PRESSED FLOWER | −0.94 | **−3.35** | −0.95 |
| AT2G34210 | AT2G34210 | | −0.76 | **−1.05** | −0.97 |
| AT2G34600 | JAZ7 | Jasmonate-zim-domain protein 7 | 0.29 | 0.03 | **1.45** |
| AT2G39240 | AT2G39240 | | −0.51 | **−1.89** | −0.93 |
| AT2G43000 | NAC042 | NAC domain containing protein 42 | **−1.03** | −0.71 | **−1.35** |
| AT2G43140 | AT2G43140 | | **−1.44** | −0.81 | **−1.91** |
| AT2G45430 | AHL22 | AT-hook motif nuclear-localized protein 22 | −0.01 | −0.08 | **−1.65** |
| AT2G45650 | AGL6 | AGAMOUS-like 6 | **3.00** | **3.16** | **3.02** |
| AT2G47810 | NF-YB5 | Nuclear factor Y, subunit B5 | −0.84 | **−2.74** | −0.62 |
| AT3G04570 | AHL19 | AT-hook motif nuclear-localized protein 19 | −0.35 | −0.46 | **−1.40** |
| AT3G10470 | AT3G10470 | | −0.87 | **−1.09** | **−2.11** |
| AT3G12977 | AT3G12977 | | −0.43 | −0.65 | **−2.23** |
| AT3G17600 | IAA31 | Indole-3-acetic acid inducible 31 | −0.69 | 0.33 | **−2.64** |
| AT3G18400 | NAC058 | NAC domain containing protein 58 | −0.08 | 0.13 | **−1.39** |
| AT3G19040 | HAF2 | Histone acetyltransferase of the TAFII250 family 2 | 0.95 | **1.19** | **1.05** |
| AT3G19184 | AT3G19184 | | −0.46 | **−1.75** | −0.18 |
| AT3G22275 | AT3G22275 | | 0.76 | 0.81 | **1.97** |
| AT3G46080 | AT3G46080 | | −0.13 | −0.09 | **−1.17** |
| AT3G49760 | bZIP5 | Basic leucine-zipper 5 | −0.25 | **−2.53** | **−1.10** |
| AT4G12050 | AT4G12050 | | −0.01 | −0.35 | **−2.12** |
| AT4G16610 | AT4G16610 | | **1.10** | −0.18 | −0.03 |
| AT4G17800 | AT4G17800 | | −0.24 | −0.23 | **−1.34** |
| AT4G18610 | LSH9 | LIGHT SENSITIVE HYPOCOTYLS 9 | −0.51 | −0.07 | **−1.10** |
| AT4G19000 | IWS2 | | 0.18 | 0.39 | **1.13** |

**Table 3** (continued)

| Gene | Name | Description | $Log_2$-fold change | | |
|---|---|---|---|---|---|
| | | | AnAXE-EV | AnRAE-EV | AnFAE-EV |
| AT4G21340 | B70 | | **−1.43** | **−3.37** | **−1.29** |
| AT4G21440 | MYB102 | MYB-like 102 | **1.14** | −0.06 | **1.18** |
| AT4G25560 | LAF1 | LONG AFTER FAR-RED LIGHT 1 | −0.42 | 0.83 | **−2.48** |
| AT4G33880 | RSL2 | ROOT HAIR DEFECTIVE 6-LIKE 2 | −0.78 | **−1.59** | **−2.77** |
| AT4G35590 | RKD5 | RWP-RK domain-containing 5 | −0.20 | −0.24 | **−3.22** |
| AT4G37940 | AGL21 | AGAMOUS-like 21 | **−2.91** | **−1.68** | **−2.01** |
| AT5G01900 | WRKY62 | WRKY DNA-binding protein 62 | **−1.09** | −0.99 | **−1.00** |
| AT5G06839 | TGA10 | TGACG (TGA) motif-binding protein 10 | −0.67 | **−1.20** | **−2.12** |
| AT5G07500 | PEI1 | | −0.31 | **1.19** | 0.85 |
| AT5G10280 | MYB92 | myb domain protein 92 | **−1.54** | −0.77 | **−1.46** |
| AT5G13220 | JAZ10 | Jasmonate-zim-domain protein 10 | 0.44 | −0.28 | **1.41** |
| AT5G14750 | MYB66 | myb domain protein 66 | **−2.05** | −0.66 | −0.34 |
| AT5G21960 | AT5G21960 | | **3.55** | **1.70** | **3.58** |
| AT5G22380 | NAC090 | NAC domain containing protein 90 | **−1.10** | **−1.65** | **−3.58** |
| AT5G24110 | WRKY30 | WRKY DNA-binding protein 30 | **−1.51** | −0.71 | −0.84 |
| AT5G24330 | ATXR6 | ARABIDOPSIS TRITHORAX-RELATED PROTEIN 6 | −0.58 | −0.31 | **−1.46** |
| AT5G42020 | BIP2 | | −0.93 | **−1.07** | **−1.03** |
| AT5G43540 | AT5G43540 | | −0.45 | −0.47 | **−2.97** |
| AT5G52830 | WRKY27 | WRKY DNA-binding protein 27 | −0.71 | −0.28 | **−1.50** |
| AT5G53950 | CUC2 | CUP-SHAPED COTYLEDON 2 | −0.49 | −0.09 | **−1.74** |
| AT5G58010 | LRL3 | LJRHL1-like 3 | 0.03 | **−1.53** | **−1.93** |
| AT5G58280 | AT5G58280 | | −0.12 | 0.32 | **−3.28** |
| AT5G65790 | MYB68 | myb domain protein 68 | −0.40 | −0.59 | **−1.17** |
| AT5G66700 | HB53 | Homeobox 53 | 0.86 | **1.32** | 0.95 |
| AT5G66870 | ASL1 | ASYMMETRIC LEAVES 2-like 1 | −0.56 | −0.52 | **−2.03** |

Bold values represent statistically significant gene expression relative to EV plants ($p < 0.05$). Underlined values indicate unique up- or down-regulation

than unique. Notably, AnAXE and AnRAE shared more metabolites with each other than with AnFAE (Fig. 4a).

All detected metabolites were arranged in a heat map using a hierarchical clustering algorithm based on normalized metabolite quantity. Metabolites with high correlation (Pearson correlation coefficient > 0.90) between AnAXE, AnRAE, and AnFAE were clustered and compared to the same metabolites in EV control plants (Fig. 4b). These clusters of highly correlated metabolites illustrate distinct differences between each transgenic line and EV. This suggests that changes occur in specific pathways in response to cell wall modification.

## Correlation of transcriptome with metabolome results in increased sensitivity of analysis

To further increase the predictive power of the analyses, transcript abundance was correlated with metabolite abundance. To perform this correlation, both entire datasets were used for analysis. The entire raw transcriptome dataset represented as FPKM, and raw metabolome dataset, represented in log abundance, were uploaded to the PMR database. As described in the methods, all transcripts were correlated with metabolite abundances across all experimental samples. Genes exceeding the correlation cutoff (Pearson correlation greater than 0.90) for each metabolite, and their associated pathways, were pooled together to provide a quantitative analysis of the pathways most perturbed in response to CW modification. The most highly enriched pathways (those associated with the highest number of metabolites) for each transgenic line are shown in Table 4. To determine the cutoff point of significance, 64 randomly chosen metabolites were correlated with transcripts to produce a randomized list of pathway enrichments (Supplementary Figure 4). Pathways exceeding the highest value from the random metabolite set were considered significantly enriched. All co-analysis results, including pathways not considered significantly enriched, are presented in Supplementary Table 4.

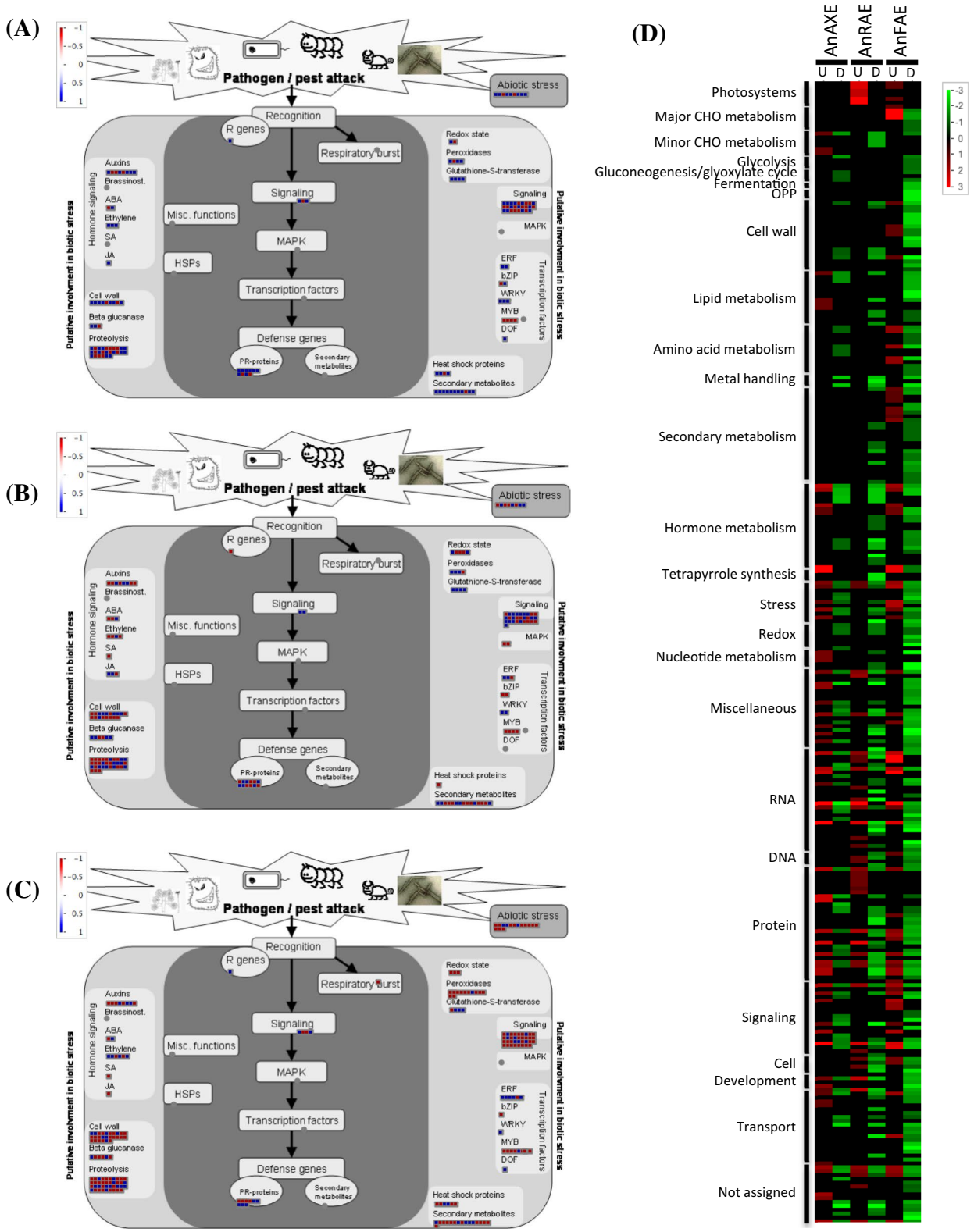


**Fig. 2** Overview of gene expression and stress responses visualized by Mapman software. **a** Stress response enrichment among DE genes in AnAXE plants. **b** Stress response enrichment among DE genes in AnRAE plants. **c** Stress response enrichment among DE genes in AnFAE plants. **d** Hierarchical clustering heat map of all DE genes showing enrichments across all lines (U = upregulated vs. EV; D = downregulated vs. EV). Scale bars display $\log_2$-fold change in transgenic lines relative to EV

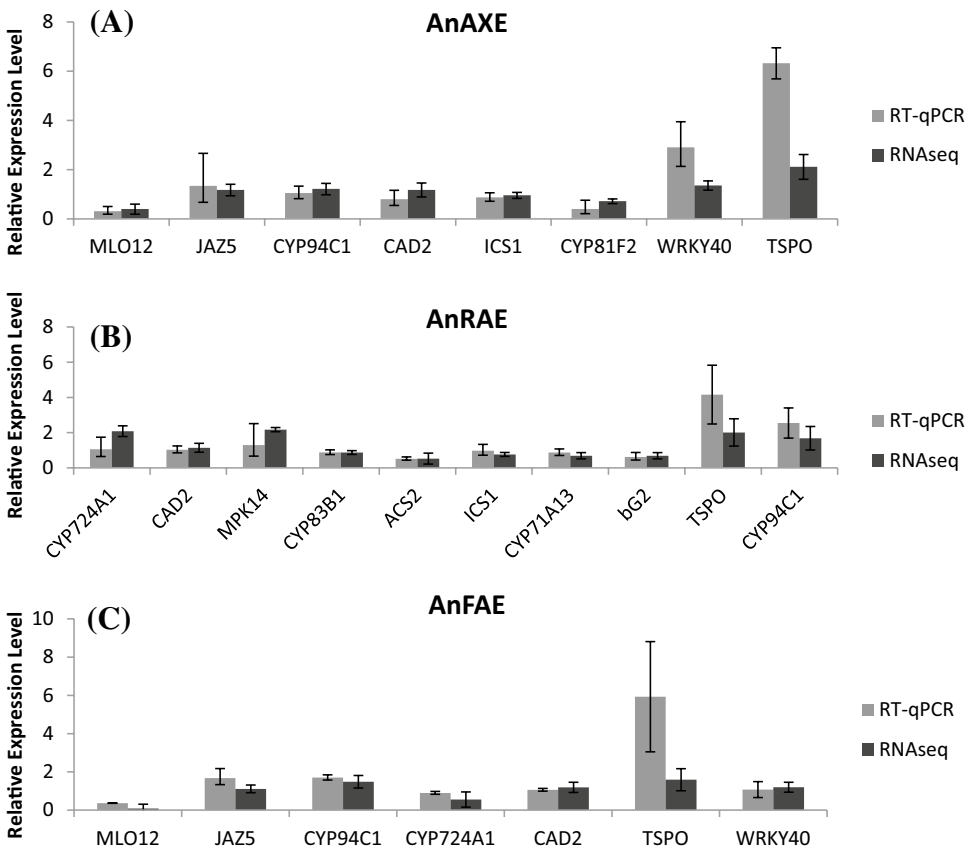


**Fig. 3** Comparison of gene expression between RNAseq and RT-qPCR. **a** gene expression analysis of AnAXE plants. **b** Gene expression analysis of AnRAE plants. **c** Gene expression analysis of AnFAE plants. FPKM fold change relative to EV was used for RNAseq, and $2^{-\Delta\Delta Cq}$ values were used for RT-qPCR

The AnAXE plants displayed enrichments in 13 pathways, including several primary metabolism pathways that are known to provide substrate for specialized metabolism associated with glucosinolates and camalexin. These pathways include adenosine nucleotides de novo biosynthesis (9 genes upregulated) and methionine salvage (2 genes upregulated). One specialized metabolic pathway, camalexin biosynthesis, was also notably enriched (3 genes upregulated, 5 genes downregulated) (Table 4).

In AnRAE plants, 53 pathways were enriched significantly. The AnRAE plants, like the AnAXE plants, showed significant enrichment in adenosine nucleotides biosynthesis (8 genes upregulated, 2 genes downregulated) and camalexin biosynthesis (3 genes upregulated, 4 genes downregulated). In contrast to AnAXE, AnRAE plants showed an enrichment of phenylalanine, tyrosine, and tryptophan biosynthesis (9 genes upregulated), and glucosinolate biosynthesis from homomethionine (2 genes upregulated). Distinct from the AnAXE plants, the S-adenosyl-methionine biosynthetic pathway was significantly downregulated in AnRAE plants (11 genes); also, 13 genes involved in ethylene biosynthesis were downregulated in AnRAE (Table 4). Additionally, 2 genes in the specialized metabolic pathway glucosinolate biosynthesis from homomethionine were upregulated.

The AnFAE plants had 20 pathways enriched in this analysis, and also showed enrichment in primary metabolism, where adenosine nucleotide biosynthesis was upregulated (8 genes). In contrast to both AnAXE and AnRAE, only one gene was upregulated involved in methionine salvage. AnFAE plants showed enrichment in downregulation of lipid biosynthesis pathways: triacylglycerol biosynthesis, wax esters biosynthesis, CDP-diacylglycerol biosynthesis, and phospholipid biosynthesis were all downregulated. In addition, the ABA biosynthesis pathway (3 genes) was downregulated (Table 4). While not considered significant, 15 genes with molecular functions of peroxidase/redox activity were downregulated in AnFAE plants (Supplementary Table 4).

## Discussion

### Transcriptome analysis reveals potential signaling components involved in defense responses and compensatory mechanisms

Previously, we have shown that Arabidopsis plants expressing AnAXE, AnRAE, and AnFAE CWDEs exhibit changes

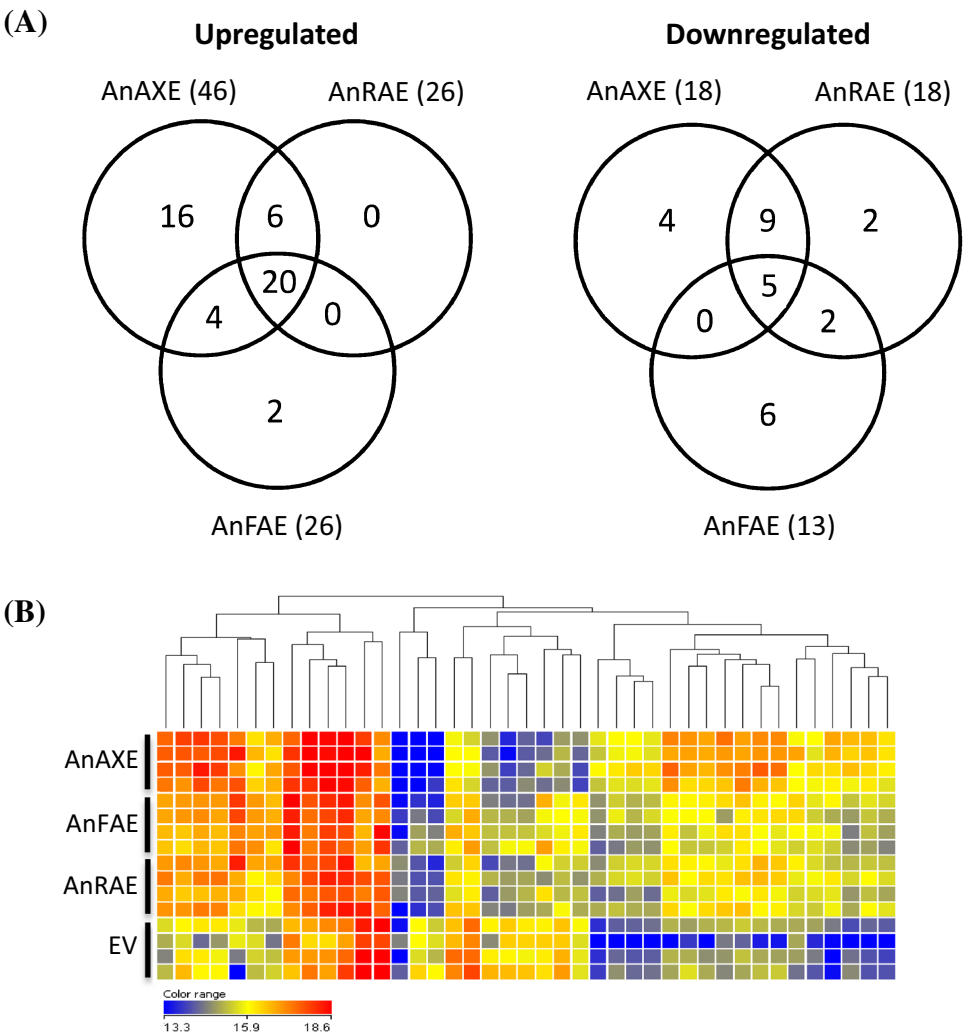


**Fig. 4** Abundance of metabolites in AnAXE, AnRAE, and AnFAE plants relative to EV. **a** Venn diagrams comparing overlap of significantly different metabolites in each transgenic line. Values in parentheses indicate total number of significant metabolites **b** Hierarchical clustering heat map of highly correlated metabolites compared to EV controls

in gene expression and defense response to pathogens. AnRAE and AnAXE plants have lower cell wall acetylation and higher resistance to the fungal necrotroph *B. cinerea* in comparison with wild type plants (Pogorelko et al. 2013), whereas AnFAE plants have reduced cell wall feruloylation and show higher susceptibility to *B. cinerea* (Reem et al. 2016; Pogorelko et al. 2011). We proposed that these changes in defense response are likely triggered by cell wall modifications caused by the introduced CWDEs. In this study, we combine transcriptome and metabolome analysis to reveal candidate signaling components in the plant response to specific cell wall modifications.

High q-values observed in the transcriptome analysis performed here were a result of a flat distribution of p-values (Supplementary Figure 1) (Nettleton et al. 2006), which is likely due to subtle changes in gene expression in each line. Since only one developmental stage of very young seedlings was chosen, it is also possible that a different timepoint or developmental stage could yield higher differential expression, which will be tested in the future. Despite this limitation, the transcriptome analysis demonstrated that each specific modification of the plant cell wall induces a relatively small but distinct set of genes. DE genes determined by transcriptome analysis are diverse and include cell wall-related genes, stress response genes, and transcription factors, but many of these genes are differentially expressed in multiple lines; a large proportion of DE genes were shared by at least, two different lines (Fig. 1).

The AnAXE plants exhibited differential expression in some known stress-related genes, including the MYB102 transcription factor, two glycosyl hydrolases, downy mildew resistance locus, two WRKY transcription factors, and an ethylene response factor. MYB102 is involved in both wounding and osmotic stresses, in particular during insect herbivory (Denekamp and Smeekens 2003; De Vos et al. 2006). The upregulation of two glycosyl hydrolases, GH9C3 and CEL3, and downregulation of a xyloglucan endotransglucosylase XTH26 could reflect a wall remodeling event in response to deacetylation of hemicelluloses in AnAXE plants. The transmembrane protein MLO12, which is

**Table 4** The most highly enriched pathways of each transgenic line after correlation of transcriptome with metabolome datasets, with a correlation cutoff of $r > 0.90$

| Enriched pathways | Number of genes upregulated | Number of genes downregulated |
|---|---|---|
| AnAXE | | |
| Aerobic respiration (cytochrome c) | 17 | 9 |
| Adenosine nucleotides de novo biosynthesis | 9 | |
| Aerobic respiration (alternative oxidase pathway) | 12 | 7 |
| NAD/NADH phosphorylation and dephosphorylation | 9 | 7 |
| Camalexin biosynthesis | 3 | 5 |
| Oxygenic photosynthesis | 17 | 4 |
| Photosynthesis light reactions | 11 | |
| S-methyl-5-thio-α-D-ribose 1-phosphate degradation | 3 | |
| Triacylglycerol degradation | 10 | |
| Methionine salvage I (bacteria and plants) | 2 | |
| Volatile benzenoid biosynthesis I (ester formation) | 2 | |
| Cytokinins 7-N-glucoside biosynthesis | | 5 |
| Cytokinins 9-N-glucoside biosynthesis | | 5 |
| Betanidin degradation | | 20 |
| Rubisco shunt | 3 | 4 |
| Superpathway of phenylalanine, tyrosine and tryptophan biosynthesis | 8 | 3 |
| Ascorbate glutathione cycle | 3 | |
| Glucosinolate biosynthesis from homomethionine | 2 | |
| AnRAE | | |
| Aerobic respiration (cytochrome c) | 16 | 13 |
| L-Glutamine biosynthesis II (tRNA-dependent) | | 1 |
| Adenosine nucleotides de novo biosynthesis | 8 | 2 |
| Oxygenic photosynthesis | 9 | 5 |
| Camalexin biosynthesis | 3 | 4 |
| 3-Dehydroquinate biosynthesis I | 1 | 1 |
| Aerobic respiration (alternative oxidase pathway) | 10 | 10 |
| Photosynthesis light reactions | 7 | |
| Triacylglycerol degradation | 13 | |
| NAD/NADH phosphorylation and dephosphorylation | 8 | 10 |
| Superpathway of phenylalanine, tyrosine and tryptophan biosynthesis | 9 | |
| Volatile benzenoid biosynthesis I (ester formation) | 2 | 1 |
| S-adenosyl-L-methionine biosynthesis | | 11 |
| Cysteine biosynthesis I | 1 | 7 |
| Seleno-amino acid biosynthesis | | 8 |
| tRNA charging | | 9 |
| Biotin biosynthesis from 7-keto-8-aminopelargonate | 1 | 1 |
| Cardiolipin biosynthesis II | 1 | 1 |
| Ethylene biosynthesis I (plants) | | 13 |
| Cytokinins degradation | | 1 |
| Methionine degradation I (to homocysteine) | | 11 |
| Tetrahydrofolate salvage from 5,10-methenyltetrahydrofolate | | 1 |
| Ubiquinol-9 biosynthesis (eukaryotic) | 1 | |
| Glucosinolate biosynthesis from homomethionine | 2 | |
| S-adenosyl-L-methionine cycle II | | 12 |
| S-methyl-5-thio-α-D-ribose 1-phosphate degradation | 2 | |
| Tryptophan biosynthesis | 7 | |
| Cadmium transport I | | 1 |
| Mevalonate pathway I | | 2 |

**Table 4** (continued)

| Enriched pathways | Number of genes upregulated | Number of genes downregulated |
|---|---|---|
| Phylloquinol biosynthesis | 1 | 1 |
| Superpathway of proto- and siroheme biosynthesis | 1 | 4 |
| Xylan biosynthesis | | 4 |
| Betanidin degradation | 2 | 20 |
| Cyclopropane and cyclopropene fatty acid biosynthesis | 1 | |
| Cyclopropane fatty acid (CFA) biosynthesis | 1 | |
| Phospholipid biosynthesis II | 4 | 6 |
| Acetyl-CoA Biotin network | | 10 |
| Calvin-Benson-Bassham cycle | 2 | 3 |
| Heme biosynthesis I | 1 | 3 |
| Tetrapyrrole biosynthesis I | 1 | 3 |
| Tyrosine biosynthesis II | 1 | 3 |
| 5-Aminoimidazole ribonucleotide biosynthesis I | | 1 |
| Abscisic acid biosynthesis | 1 | 3 |
| CDP-diacylglycerol biosynthesis I | | 3 |
| CDP-diacylglycerol biosynthesis II | | 3 |
| Cellulose biosynthesis | | 3 |
| Cytokinins 7-N-glucoside biosynthesis | | 4 |
| Cytokinins 9-N-glucoside biosynthesis | | 4 |
| Methionine salvage I (bacteria and plants) | 2 | |
| Pyruvate fermentation to lactate | | 1 |
| Triacylglycerol biosynthesis | | 5 |
| Vestitol and sativan biosynthesis | 2 | |
| Wax esters biosynthesis I | | 6 |
| AnFAE | | |
| Aerobic respiration (cytochrome c) | 15 | 9 |
| Adenosine nucleotides de novo biosynthesis | 8 | |
| Camalexin biosynthesis | 3 | 4 |
| Oxygenic photosynthesis | 8 | |
| Photosynthesis light reactions | 6 | |
| Aerobic respiration (alternative oxidase pathway) | 10 | 7 |
| NAD/NADH phosphorylation and dephosphorylation | 9 | 7 |
| Triacylglycerol degradation | 10 | |
| S-methyl-5-thio-α-D-ribose 1-phosphate degradation | 1 | |
| Volatile benzenoid biosynthesis I (ester formation) | 2 | |
| Pyruvate fermentation to lactate | | 1 |
| Triacylglycerol biosynthesis | | 5 |
| Wax esters biosynthesis I | | 6 |
| CDP-diacylglycerol biosynthesis I | | 3 |
| CDP-diacylglycerol biosynthesis II | | 3 |
| Cytokinins 7-N-glucoside biosynthesis | | 4 |
| Cytokinins 9-N-glucoside biosynthesis | | 4 |
| Abscisic acid biosynthesis | | 3 |
| Methionine salvage I (bacteria and plants) | 1 | |
| Phospholipid biosynthesis II | | 6 |
| Peroxidase activity | | 15 |

downregulated in AnAXE plants, is important for resistance to fungus via interaction with tryptophan-derived metabolites (Consonni et al. 2010). The expression of chitinase A, a gene which is induced specifically under wounding and salt stress (Takenaka et al. 2009), was also upregulated in AnAXE, suggesting it plays a role in the enhanced disease resistance seen in these plants (Pogorelko et al. 2013).

Both the AnAXE and AnRAE lines have upregulated PDF1.2b and PDF1.4, important defensins often upregulated during pathogenesis (Penninckx et al. 1998; Thomma et al. 2002). TSPO, a tryptophan-rich membrane protein, and two transcription factors (bZIP48 and NAC090), are also upregulated in both lines. Since both lines have reduced cell wall acetylation and increased resistance to *B. cinerea*, it is plausible that these genes are some of the key players in the defense responses induced in these plants by the cell wall modification. However, more analysis on these genes must be done in the future to determine their role in defense response of AnAXE and AnRAE plants. The downregulation of transcription factors bZIP5, MYB54, and MYB61 in AnRAE plants, but not in AnAXE plants, could reflect the subtle differences (Pogorelko et al. 2013) in defense responses between AnAXE and AnRAE plants.

The AnFAE plants displayed more unique gene expression patterns relative to AnAXE and AnRAE plants. This may reflect that the AnFAE plants, in contrast with AnAXE/AnRAE, have compromised resistance to *B. cinerea* (Reem et al. 2016). However, some defense response genes are upregulated in AnFAE plants, indicating that the plants may attempt to compensate for the weakness of their cell walls associated with the reduction in cross-linking via ferulate (Reem et al. 2016). For example, the fungal defense response genes PDF1.2, 1.2B, and 1.3 (Thomma et al. 2002; Pré et al. 2008) are upregulated in the AnFAE plants. The upregulation of JAZ genes in the AnFAE plants suggests an inhibition of JA response, consistent with the higher susceptibility of these plants to fungal necrotrophs.

Members of a large family of transcription factors, WRKY26, WRKY61, WRKY62, and WRKY65 were all downregulated in the AnFAE plants. WRKY62 interacts with WRKY38 and histone deacetylase 19 in Arabidopsis as a transcriptional regulator of defense response (Kim et al. 2008). Since WRKY transcription factors are involved in a variety of defense responses, it is possible that the downregulation of these genes reflects the compromised defense response seen in the AnFAE plants (Reem et al. 2016).

The downregulation of extensin and extensin-like genes in AnFAE (but not in AnAXE or AnRAE) suggests a plant response associated with the reduced level of wall-bound ferulate, which has been hypothesized to interact with extensin proteins (Qi et al. 1995; Reem et al. 2016). Downregulation of the feruloyl transferase RWP1 (Gou et al. 2009; Molina et al. 2009) in the AnFAE plants is perhaps also associated with the reduction of wall feruloylation in this line.

While RNA-Seq alone is a powerful tool, we find that correlation of RNA-Seq with metabolome datasets leads to increased sensitivity of DE gene selection and allows identification of genes that would not normally be considered significant through transcriptomics alone. Correlation of transcriptome with the metabolome datasets enabled us to determine the most highly enriched pathways up- or downregulated in each transgenic line. These correlation analyses indicate that several pathways are consistently enriched in each transgenic line. Notably, co-analyses revealed a substantial number of primary metabolic pathways, illustrating the significant shifts in cell metabolism associated with cell wall-mediated defense responses.

## Correlation analysis reveals partially overlapping responses of the AnAXE and AnRAE plants exhibiting decreased susceptibility to *B. cinerea*

The AnAXE and AnRAE transcriptome and metabolome showed similar patterns of differentially expressed pathways in comparison with control plants. Both exhibited upregulation in metabolites and genes of primary metabolic pathways, specifically, de novo biosynthesis of adenosine nucleotides, aerobic respiration, NAD/NADH phosphorylation, and triacylglycerol degradation.

Perhaps due to the more extreme defense response phenotype (Pogorelko et al. 2013), many more pathways were affected in the AnRAE plants than in AnAXE. These pathways included specialized metabolism for defense response, such as glucosinolate biosynthesis and aromatic amino acids (tryptophan) biosynthesis (Table 4).

Adenosine nucleotides biosynthesis is an important pathway for ATP production. Aromatic amino acids such as phenylalanine, tyrosine, and tryptophan are essential precursors of cell wall components and serve as substrates for the defense response compounds, the aromatic and indole glucosinolates and camalexin (Grubb and Abel 2006). Aliphatic glucosinolates are important defense metabolites derived directly from methionine (Field et al. 2004), and the methionine salvage pathway is upregulated in AnAXE plants, while methionine degradation is downregulated in AnRAE plants. Upregulation of synthesis of adenosine nucleotides suggests that the AnAXE and AnRAE plants have increased production of ATP, which could serve as cofactor for the numerous catalytic reactions occurring in a cell at any given time. An enrichment of biosynthesis of aromatic amino acids and glucosinolate biosynthesis was observed exclusively in AnRAE plants, suggesting that these two pathways contribute to the difference in defense response between AnRAE and AnAXE plants. These enrichment analyses illustrate the high demand that defense responses places on primary metabolism. They

also show how similar defense response phenotypes seen in AnAXE and AnRAE can manifest themselves through partially overlapping metabolic pathways.

The AnAXE plants exhibited upregulation of genes in the methionine biosynthesis pathway, whereas AnRAE plants showed downregulation of genes involved in SAM and ethylene biosynthesis. Because SAM, a common one-carbon donor, is involved in many biochemical reactions, the significance of this finding is not clear. SAM is required for biosynthesis of the methyl jasmonate, and is a precursor for ethylene production (Yang and Hoffman 1984). Reduced expression of SAM biosynthetic genes in the AnRAE plants could affect the types and levels of defense metabolites formed in the cells. Additionally, the defense signaling induced by reduced CW acetylation due to AnRAE expression might be modified by reduction of ethylene biosynthesis, since 13 genes involved in ethylene biosynthesis were downregulated in these plants (Table 4). In the AnAXE plants, the upregulation of genes in the methionine biosynthesis pathway (but no changes in SAM biosynthesis) likely indicates a more balanced ratio of SAM-dependent—SAM-independent metabolites than in AnRAE plants, where SAM biosynthesis is downregulated. However, more experiments are necessary to confirm this hypothesis.

### Correlation analysis provides insight into cell wall remodeling in the AnFAE plants due to reduced feruloylation which leads to compromised defense

The correlation analysis of transcriptome and metabolome in AnFAE plants revealed downregulation of genes belonging to several pathways involved in fatty acid biosynthesis. Among those are wax esters biosynthesis I, CDP-diacylglycerol biosynthesis I & II, phosphatidylglycerol biosynthesis I & II, triacylglycerol biosynthesis, and phospholipid biosynthesis II (Table 4). It has been shown that ferulic acid is covalently bound to cutin and suberin waxes in Arabidopsis and other species (Gou et al. 2009; Molina et al. 2009). Downregulation of the wax ester biosynthesis pathway shown in AnFAE suggests possible sensing and feedback regulation of extracellular ferulic acid. In this case, an extracellular sensor might detect ferulate-lacking portions of cutin and downregulate biosynthesis of new cuticle until more ferulic acid can bind.

Lipids also serve as signaling molecules, or precursors of signaling molecules (Walley et al. 2013). One well-known example, jasmonic acid, is derived in part from galactolipids, which have been hydrolyzed to alpha-linolenic acid (Wasternack 2007). Studies of fatty acid levels in the arbuscular-mycorrhizal fungi *Glomus intraradices* and *Gigaspora rosea* have shown these fungi depend on host production of palmitic acid for fungal fatty acid elongation to occur (Trépanier et al. 2005). Other studies indicate that an increase in 16:1 fatty acid in eggplant increased resistance to *Verticillium dahlia* (Xing and Chin 2000). The downregulation of lipid biosynthesis observed in the AnFAE plants might be a mechanism intended to prevent specific fungal species from benefiting from plant fatty acids.

While not considered significant by our metrics, correlation of metabolite abundance with gene expression in the AnFAE plants uncovered downregulation of 15 peroxidase enzymes related to lignin biosynthesis and of several extensin biosynthesis related genes (Supplementary Table 4). Because peroxidases are important contributors to cell wall strength and maintenance, it is worth considering peroxidase action as it pertains to CWI. Usually, plants fortify their cell walls by accumulating wall-bound lignin and extensins in response to pathogen invasion, and peroxidases are critical for this action (Mikulic Petkovšek et al. 2008; Lamport et al. 2011). AnFAE plants possess significantly reduced amounts of loosely associated HF-soluble extensin, but no significant reduction of total extensin (Reem et al. 2016). This reduction of soluble, non-cross-linked extensin in the AnFAE plants correlates with the downregulation of extensin related genes observed in this study. We did not observe significant difference in total lignin content in AnFAE plants (Supplementary Figure 4), however, reduction of peroxidases might affect lignin's degree of polymerization, thus weakening cell walls and decreasing resistance to fungal penetration in the AnFAE plants.

## Conclusions

The combined transcriptome and metabolome analysis in plants altered in cell wall acetyl and feruloyl content has provided insight into the cell wall-mediated mechanisms involved in biotic stress response. Our data indicate that through changes in cell wall components, plants are able to initiate compensatory responses. Plants expressing AnAXE and AnRAE, both of which have reduced cell wall acetylation (Pogorelko et al. 2013), exhibit partially overlapping defense responses. AnFAE plants, which have decreased cell wall feruloylation (Reem et al. 2016), show distinct changes in defense responses. We have uncovered sets of transcription factors, wall-related genes, and stress response genes that are likely candidates in plant response to each cell wall alteration. Additionally, the data reveal the demand that specialized metabolism exerts on primary metabolism in order to produce metabolites associated with cell wall-mediated defense response. These results illustrate the complexity of signaling induced by cell wall modifications and the robustness of extracellular sensing mechanisms in plants.

The results obtained in this study point to a potential utility of the post-synthetic modification of cell wall

properties in elucidating key genes/pathways in cell wall integrity signaling induced in response to these modifications. Hydrolytic enzymes are the key components involved in cell wall remodeling, the main mechanism of cell wall adjustments during plant development, and response to environmental cues. Therefore, employment of such enzymes with well characterized specificities, overexpression of which in the plant apoplast causes particular modifications in polysaccharide structures or their cross-linking, represents a promising approach for studying plant responses to these modifications. In addition, reduction of the degree of polysaccharide acetylation can subsequently increase their accessibility to glycosidases, as was shown for AnAXE and AnRAE plants (Pogorelko et al. 2013), which can potentially release oligosaccharides involved in CWI control. All such cell wall modifications, mimicking the action of pathogen CWDEs, initiate responsive pathways potentially involved in CWI signaling during pathogenesis, and thus, impact plant resistance to biotic stresses. Therefore, action of CWDEs expressed in the plant apoplast can assist in dissecting the pathways usually initiated in response to complex cell wall modifications caused by the mixture of CWDEs secreted all together during pathogenesis. These results demonstrate that the correlation analysis of global transcriptome and metabolome data increases the power of the predictions in investigation and uncovering novel components involved in signaling induced by cell wall integrity alterations in response to environmental stresses.

**Acknowledgements** This research was in part supported by the NSF-MCB (National Science Foundation) (Grant #1121163 to OAZ) and USDA-NIFA (National Institute of Food and Agriculture) (Grant #2015-07802 to OAZ). The authors thank Zebulun Arendsee (Iowa State University) for his assistance in bioinformatics analysis.

**Author contributions** NTR conducted all analyses of transcriptome and metabolome datasets, and wrote the paper. OZ and LL designed the experiments and wrote the paper. XZ cleaned and mapped reads, and applied statistical analysis to transcriptome data. HC and XL conducted metabolite analysis. MH and ESW developed and maintain the PMR database and statistical analyses and contributed to the paper.

## References

Asai T, Tena G, Plotnikova J, Willmann MR, Chiu W-L, Gomez-Gomez L, Boller T, Ausubel FM, Sheen J (2002) MAP kinase signalling cascade in Arabidopsis innate immunity. Nature 415:977–983. https://doi.org/10.1038/415977a

Bellincampi D, Cervone F, Lionetti V (2014) Plant cell wall dynamics and wall-related susceptibility in plant–pathogen interactions. Front Plant Sci 5:1–8. https://doi.org/10.3389/fpls.2014.00228

Boller T, He SY (2009) Innate immunity in plants: an arms race between pattern recognition receptors in plants and effectors in microbial pathogens. Science 324:742–744. https://doi.org/10.1126/science.1171647

Brutus A, Sicilia F, Macone A, Cervone F, Lorenzo G, De (2010) A domain swap approach reveals a role of the plant wall-associated kinase 1 (WAK1) as a receptor of oligogalacturonides. Proc Natl Acad Sci USA. https://doi.org/10.1073/pnas.1000675107. http://www.pnas.org/cgi

Consonni C, Bednarek P, Humphry M, Francocci F, Ferrari S, Harzen A, van Themaat EVL, Panstruga R (2010) Tryptophan-derived metabolites are required for antifungal defense in the Arabidopsis mlo2 mutant. Plant Physiol 152:1544–1561. https://doi.org/10.1104/pp.109.147660

De Vos M, Denekamp M, Dicke M, Vuylsteke M, Van Loon L, Smeekens SC, Pieterse CM (2006) The *Arabidopsis thaliana* transcription factor AtMYB102 functions in defense against the insect herbivore *Pieris rapae*. Plant Signal Behav 1:305–311

De Lorenzo G, Brutus A, Savatin DV, Sicilia F, Cervone F (2011) Engineering plant resistance by constructing chimeric receptors that recognize damage-associated molecular patterns (DAMPs). FEBS Lett 585:1521–1528. https://doi.org/10.1016/j.febslet.2011.04.043

de Jonge R, van Esse HP, Maruthachalam K, Bolton MD, Santhanam P, Saber MK, Zhang Z, Usami T, Lievens B, Subbarao KV, Thomma BPHJ (2012) Tomato immune receptor Ve1 recognizes effector of multiple fungal pathogens uncovered by genome and RNA sequencing. Proc Natl Acad Sci USA 109:5110–5115. https://doi.org/10.1073/pnas.1119623109

De Cremer K, Mathys J, Vos C, Froenicke L, Michelmore RW, Cammue BPA, De Coninck B (2013) RNAseq-based transcriptome analysis of *Lactuca sativa* infected by the fungal necrotroph *Botrytis cinerea*. Plant Cell Environ 36:1992–2007. https://doi.org/10.1111/pce.12106

Denekamp M, Smeekens SC (2003) Integration of wounding and osmotic stress signals determines the expression of the AtMYB102 transcription factor gene. Plant Physiol 132:1415–1423. https://doi.org/10.1104/PP.102.019273

Ehlting J, Chowrira SG, Mattheus N, Aeschliman DS, Arimura G-I, Bohlmann J (2008) Comparative transcriptome analysis of *Arabidopsis thaliana* infested by diamond back moth (*Plutella xylostella*) larvae reveals signatures of stress response, secondary metabolism, and signalling. BMC Genom 9:154. https://doi.org/10.1186/1471-2164-9-154

Engelsdorf T, Hamann T (2014) An update on receptor-like kinase involvement in the maintenance of plant cell wall integrity. Ann Bot 114:1339–1347. https://doi.org/10.1093/aob/mcu043

Ferrari S, Savatin DV, Sicilia F, Gramegna G, Cervone F, De Lorenzo G (2013) Oligogalacturonides: plant damage-associated molecular patterns and regulators of growth and development. Front Plant Sci 4:49. https://doi.org/10.3389/fpls.2013.00049

Field B, Cardon G, Traka M, Botterman J, Vancanneyt G, Mithen R (2004) Glucosinolate and amino acid biosynthesis. Plant Physiol 135:828–839. https://doi.org/10.1104/pp.104.039347.828

Godfrey D, Rathjen JP (2012) Recognition and response in plant PAMP-triggered immunity. Wiley, Chichester

Gou J, Yu X, Liu C (2009) A hydroxycinnamoyltransferase responsible for synthesizing suberin aromatics in Arabidopsis. Proc Natl Acad Sci USA 106:18855–18860

Gramegna G, Modesti V, Savatin DV, Sicilia F, Cervone F, De Lorenzo G (2016) GRP-3 and KAPP, encoding interactors of WAK1, negatively affect defense responses induced by oligogalacturonides and local response to wounding. J Exp Bot 67:1715–1729. https://doi.org/10.1093/jxb/erv563

Grubb CD, Abel S (2006) Glucosinolate metabolism and its control. Trends Plant Sci 11:89–100. https://doi.org/10.1016/j.tplants.2005.12.006

Guo H, Li L, Ye H, Yu X, Algreen A, Yin Y (2009) Three related receptor-like kinases are required for optimal cell elongation in *Arabidopsis thaliana*. Proc Natl Acad Sci USA 106:7648–7653. https://doi.org/10.1073/pnas.0812346106

Hamann T (2012) Plant cell wall integrity maintenance as an essential component of biotic stress response mechanisms. Front Plant Sci 3:77. https://doi.org/10.3389/fpls.2012.00077

Hamann T, Denness L (2011) Cell wall integrity maintenance in plants: lessons to be learned from yeast? Plant Signal Behav 6:1706–1709. https://doi.org/10.4161/psb.6.11.17782

Hamann T, Bennett M, Mansfield J, Somerville C (2009) Identification of cell-wall stress as a hexose-dependent and osmosensitive regulator of plant responses. Plant J 57:1015–1026. https://doi.org/10.1111/j.1365-313X.2008.03744.x

Hématy K, Sado P, Van Tuinen A, Rochange S, Desnos T, Balzergue S, Pelletier S, Renou J, Höfte H (2007) A receptor-like kinase mediates the response of Arabidopsis cells to the inhibition of cellulose synthesis. Curr Biol 17:922–931. https://doi.org/10.1016/j.cub.2007.05.018

Hur M, Campbell AA, Almeida-de-Macedo M, Li L, Ransom N, Jose A, Crispin M, Nikolau BJ, Wurtele ES (2013) A global approach to analysis and interpretation of metabolic data for plant natural product discovery. Nat Prod Rep 30:565. https://doi.org/10.1039/c3np20111b

Kim K-C, Lai Z, Fan B, Chen Z (2008) Arabidopsis WRKY38 and WRKY62 transcription factors interact with histone deacetylase 19 in basal defense. Plant Cell 20:2357–2371. https://doi.org/10.1105/tpc.107.055566

Kohorn BD (2016) Cell wall-associated kinases and pectin perception. J Exp Bot 67:489–494

Kohorn BD, Kohorn SL, Saba NJ, Martinez VM (2014) Requirement for pectin methyl esterase and preference for fragmented over native pectins for wall-associated kinase-activated, EDS1/PAD4-dependent stress response in Arabidopsis. J Biol Chem 289:18978–18986. https://doi.org/10.1074/jbc.M114.567545

Kohorn BD, Hoon D, Minkoff BB, Sussman MR, Kohorn SL (2016) Rapid oligo-galacturonide induced changes in protein phosphorylation in Arabidopsis. Mol Cell Proteom 15:1351–1359. https://doi.org/10.1074/mcp.M115.055368

Kubicek CP, Starr TL, Glass NL (2014) Plant cell wall-degrading enzymes and their secretion in plant–pathogenic fungi. Annu Rev Phytopathol. https://doi.org/10.1146/annurev-phyto-102313-045831

Laluk K, Mengiste T (2010) Necrotroph attacks on plants: wanton destruction or covert extortion? Arab B 8:e0136. https://doi.org/10.1199/tab.0136

Lamport DTa, Kieliszewski MJ, Chen Y, Cannon MC (2011) Role of the extensin superfamily in primary cell wall architecture. Plant Physiol 156:11–19. https://doi.org/10.1104/pp.110.169011

Li L, Zheng W, Zhu Y, Ye H, Tang B, Arendsee ZW, Jones D, Li R, Ortiz D, Zhao X, Du C, Nettleton D, Scott MP, Salas-Fernandez MG, Yin Y, Wurtele ES (2015) QQS orphan gene regulates carbon and nitrogen partitioning across species via NF–YC interactions. Proc Natl Acad Sci USA 112:14734–14739. https://doi.org/10.1073/pnas.1514670112

Lionetti V, Raiola A, Cervone F, Bellincampi D (2014) Transgenic expression of pectin methylesterase inhibitors limits tobamovirus spread in tobacco and Arabidopsis. Mol Plant Pathol 15:265–274. https://doi.org/10.1111/mpp.12090

Liu Q, Wang X, Tzin V, Romeis J, Peng Y, Li Y (2016) Combined transcriptome and metabolome analyses to understand the dynamic responses of rice plants to attack by the rice stem borer *Chilo suppressalis* (Lepidoptera: Crambidae). BMC Plant Biol 16:259. https://doi.org/10.1186/s12870-016-0946-6

Lund SP, Division SE, Mccarthy DJ, Smyth GK, Hall E, Nettleton D (2012) Detecting differential expression in RNA-sequence data using quasi-likelihood with shrunken dispersion estimates detecting differential expression in RNA-sequence data using quasi-likelihood with shrunken dispersion estimates. Stat Appl Genet Mol Biol. https://doi.org/10.1515/1544-6115.1826

Ma Y, Walker RK, Zhao Y, Berkowitz GA (2012) Linking ligand perception by PEPR pattern recognition receptors to cytosolic $Ca^{2+}$ elevation and downstream immune signaling in plants. Proc Natl Acad Sci USA 109:19852–19857. https://doi.org/10.1073/pnas.1205448109

Mikulic Petkovšek M, Stampar F, Veberic R (2008) Increased phenolic content in apple leaves infected with the apple scab pathogen. J Plant Pathol 90:49–55

Molina I, Li-beisson Y, Beisson F, Ohlrogge JB, Pollard M (2009) Identification of an Arabidopsis feruloyl-coenzyme A transferase required for suberin synthesis. Plant Physiol 151:1317–1328. https://doi.org/10.1104/pp.109.144907

Murashige T, Skoog F (1962) A revised medium for rapid growth and bio assays with tobacco tissue cultures. Physiol Plant 15:473–497. https://doi.org/10.1111/j.1399-3054.1962.tb08052.x

Nafisi M, Stranne M, Fimognari L, Atwell S, Martens HJ, Pedas PR, Hansen SF, Nawrath C, Scheller HV, Kliebenstein DJ, Sakuragi Y (2015) Acetylation of cell wall is required for structural integrity of the leaf surface and exerts a global impact on plant stress responses. Front Plant Sci 6:1–13. https://doi.org/10.3389/fpls.2015.00550

Navarro L, Zipfel C, Rowland O, Keller I, Robatzek S, Boller T, Jones JDG (2004) The transcriptional innate immune response to flg22. Interplay and overlap with Avr gene-dependent defense responses and bacterial pathogenesis. Plant Physiol 135:1113–1128. https://doi.org/10.1104/pp.103.036749

Nettleton D, Hwang JTG, Caldo RA, Wise RP (2006) Estimating the number of true null hypotheses from a histogram of p values. J Agric Biol Environ Stat 11:337–356. https://doi.org/10.1198/108571106X129135

Penninckx IA, Thomma BP, Buchala A, Métraux JP, Broekaert WF (1998) Concomitant activation of jasmonate and ethylene response pathways is required for induction of a plant defensin gene in Arabidopsis. Plant Cell 10:2103–2113. https://doi.org/10.1105/TPC.10.12.2103

Pogorelko G, Fursova O, Lin M, Pyle E, Jass J, Zabotina OA (2011) Post-synthetic modification of plant cell walls by expression of microbial hydrolases in the apoplast. Plant Mol Biol 77:433–445. https://doi.org/10.1007/s11103-011-9822-9

Pogorelko G, Lionetti V, Fursova O, Sundaram RM, Qi M, Whitham SA, Bogdanove AJ, Bellincampi D, Zabotina OA (2013) *Arabidopsis* and *Brachypodium distachyon* transgenic plants expressing *Aspergillus nidulans* Acetylesterases have decreased degree of polysaccharide acetylation and increased resistance to pathogens. Plant Physiol 162:9–23. https://doi.org/10.1104/pp.113.214460

Popper ZA, Fry SC (2003) Primary cell wall composition of bryophytes and charophytes. Ann Bot 91:1–12. https://doi.org/10.1093/aob/mcg013

Pré M, Atallah M, Champion A, De Vos M, Pieterse CMJ, Memelink J (2008) The AP2/ERF domain transcription factor ORA59 integrates jasmonic acid and ethylene signals in plant defense. Plant Physiol 147:1347–1357. https://doi.org/10.1104/pp.108.117523

Qi X, Behrens BX, West PR, Mort AJ (1995) Solubilization and partial characterization of extensin fragments from cell walls of cotton suspension cultures. Evidence for a covalent cross-link between extensin and pectin. Plant Physiol 108:1691–1701. https://doi.org/10.1104/pp.108.4.1691

Rasmussen S, Barah P, Suarez-rodriguez MC, Bressendorff S, Friis P, Costantino P, Bones AM, Nielsen HB, Mundy J (2013) Transcriptome responses to combinations of stresses in Arabidopsis. Plant Physiol 161:1783–1794. https://doi.org/10.1104/pp.112.210773

Reem NT, Pogorelko G, Lionetti V, Chambers L, Held MA, Bellincampi D, Zabotina OA (2016) Decreased polysaccharide feruloylation compromises plant cell wall integrity and increases susceptibility to necrotrophic fungal pathogens. Front Plant Sci 7:1–21. https://doi.org/10.3389/fpls.2016.00630

Ringli C (2010) Monitoring the outside: cell wall-sensing mechanisms. Plant Physiol 153:1445–1452. https://doi.org/10.1104/pp.110.154518

Rodicio R, Heinisch JJ (2010) Together we are strong-cell wall integrity sensors in yeasts. Yeast 27:531–540. https://doi.org/10.1002/yea.1785

Savatin DV, Gramegna G, Modesti V, Cervone F (2014) Wounding in the plant tissue: the defense of a dangerous passage. Front Plant Sci 5:470. https://doi.org/10.3389/fpls.2014.00470

Schmittgen TD, Livak KJ (2008) Analyzing real-time PCR data by the comparative CT method. Nat Protoc 3:1101–1108. https://doi.org/10.1038/nprot.2008.73

Shen X, Wang Z, Song X, Xu J, Jiang C, Zhao Y, Ma C, Zhang H (2014) Transcriptomic profiling revealed an important role of cell wall remodeling and ethylene signaling pathway during salt acclimation in Arabidopsis. Plant Mol Biol 86:303–317. https://doi.org/10.1007/s11103-014-0230-9

Strauch RC, Svedin E, Dilkes B, Chapple C, Li X (2015) Discovery of a novel amino acid racemase through exploration of natural variation in *Arabidopsis thaliana*. Proc Natl Acad Sci USA 112:11726–11731. https://doi.org/10.1073/pnas.1503272112

Takenaka Y, Nakano S, Tamoi M, Sakuda S, Fukamizo T (2009) Chitinase gene expression in response to environmental stresses in *Arabidopsis thaliana*: chitinase inhibitor allosamidin enhances stress tolerance. Biosci Biotechnol Biochem 73:1066–1071. https://doi.org/10.1271/bbb.80837

Tang W, Kim T-W, Oses-Prieto JA, Sun Y, Deng Z, Zhu S, Wang R, Burlingame AL, Wang Z-Y (2008) BSKs mediate signal transduction from the receptor kinase BRI1 in Arabidopsis. Science 321:557–560. https://doi.org/10.1126/science.1156973

Thomma BPHJ, Bruno A, Cammue PA, Thevissen K (2002) Plant defensins. Planta 216:193–202. https://doi.org/10.1007/s00425-002-0902-6

Trapnell C, Pachter L, Salzberg SL (2009) TopHat: discovering splice junctions with RNA-SEq. Bioinformatics 25:1105–1111. https://doi.org/10.1093/bioinformatics/btp120

Trépanier M, Bécard G, Moutoglis P, Willemot C, Gagné S, Avis TJ, Rioux J-A (2005) Dependence of arbuscular-mycorrhizal fungi on their plant host for palmitic acid synthesis. Appl Environ Microbiol 71:5341–5347. https://doi.org/10.1128/AEM.71.9.5341-5347.2005

Tsai AYL, Chan K, Ho CY, Canam T, Capron R, Master ER, Bräutigam K (2017) Transgenic expression of fungal accessory hemicellulases in *Arabidopsis thaliana* triggers transcriptional patterns related to biotic stress and defense response. PLoS ONE 12:e0173094. https://doi.org/10.1371/journal.pone.0173094

Underwood W (2012) The plant cell wall: a dynamic barrier against pathogen invasion. Front Plant Sci 3:85. https://doi.org/10.3389/fpls.2012.00085

Voxeur A, Hofte H (2016) Cell wall integrity signaling in plants: "to grow or not to grow that's the question". Glycobiology 1:1–11. https://doi.org/10.1093/glycob/cww029

Wagner TA, Kohorn BD (2001) Wall-associated kinases are expressed throughout plant development and are required for cell expansion. Plant Cell 13:303–318. https://doi.org/10.1105/TPC.13.2.303

Walley JW, Kliebenstein DJ, Bostock RM, Dehesh K (2013) Fatty acids and early detection of pathogens. Curr Opin Plant Biol 16:520–526. https://doi.org/10.1016/j.pbi.2013.06.011

Wasternack C (2007) Jasmonates: an update on biosynthesis, signal transduction and action in plant stress response, growth and development. Ann Bot 100:681–697. https://doi.org/10.1093/aob/mcm079

Wolf S, Hématy K, Höfte H (2012) Growth control and cell wall signaling in plants. Annu Rev Plant Biol 63:381–407. https://doi.org/10.1146/annurev-arplant-042811-105449

Wu S, Shan L, He P (2014) Microbial signature-triggered plant defense responses and early signaling mechanisms. Plant Sci 228:118–126. https://doi.org/10.1016/j.plantsci.2014.03.001

Xing J, Chin C-K (2000) Modification of fatty acids in eggplant affects its resistance to Verticilliumdahliae. Physiol Mol Plant Pathol 56:217–225. https://doi.org/10.1006/pmpp.2000.0268

Xu Z, Wang M, Shi D, Zhou G, Niu T, Hahn MG, O'Neill MA, Kong Y (2017) DGE-seq analysis of MUR3-related Arabidopsis mutants provides insight into how dysfunctional xyloglucan affects cell elongation. Plant Sci 258:156–169. https://doi.org/10.1016/j.plantsci.2017.01.005

Yang S, Hoffman N (1984) Ethylene biosynthesis and its regulation in higher plants. Annu Rev Plant Physiol 35:155–189. https://doi.org/10.1146/annurev.pp.35.060184.001103